Analysis of Hubble Legacy Archive Astrometric Header Information

Michael A. Wolfe and Stefano Casertano

ABSTRACT

Astrometric information is put into the headers of the final drizzled images produced by the Hubble Legacy Archive. How well the astrometric information is sensical across all of the final drizzled images is the main thrust of this investigation. Datasets from external observations were exclusively used in this analysis. Comparisons were made between the astrometric information extracted from the final drizzled image headers and the total root mean square ranges for both Guide Star Catalogue I and Guide Star Catalogue II and the total root mean square value for the Sloan Digital Sky Survey. The results from this comparison show that the information captured from the headers is indeed reasonable as the astrometric values fall within the ranges and are above the upper limits for Guide Star Catalogue I and Guide Star Catalogue II and greater than the total root mean square of the Sloan Digital Sky Survey. Histograms were created using the offsets and root mean squares of the right ascension and declination that have been added in quadrature. The histograms of the total root mean square show extended tails with large bin numbers. A thorough visual inspection of randomly picked datasets in these extended regions and in regions around the central peak were tested to see whether the datasets either "passed", "failed" or were "undecided".

1. Introduction

The Hubble Legacy Archive (HLA) produces combined drizzled images from Hubble Space Telescope (HST) photometric observations[1] that have astrometric information in each science header. Only external observations were used in this analysis *i.e.*, dark, bias, iflat, uflat, vflat, kspot, and ecal observations for Wide Field Planetary Camera 2 (WFPC2) were excluded with analogous exemptions for the Advanced Camera for Surveys (ACS). Due to the uncertainties in the positions of the guide stars used when making photometric observations the absolute astrometry for HST images have typical errors of $1''$ - $2''$ for data taken prior to Cycle 15 (MJD $<$ 53917.0, July 1, 2006). Prior to Cycle 15 the Guide Star Catalog I (GSC I), quotes Russell et al. (1990), has an overall astrometric error range per coordinate of $0.20''$ - $0.80''$. For Cycle 15 and subsequent cycles (MJD $\geq$ 53917.0) GSC I, now Guide Star Catalog II (GSC II), was updated and has better

[1]Based on observations made with the NASA/ESA Hubble Space Telescope, and obtained from the Hubble Legacy Archive, which is a collaboration between the Space Telescope Science Institute (STScI/NASA), the Space Telescope European Coordinating Facility (ST-ECF/ESA) and the Canadian Astronomy Data Centre (CADC/NRC/CSA).

astrometry with a typical error per coordinate, depending on magnitude, between 0.20″ - 0.28″ (Lasker et al. 2008). When adding the aforementioned astrometric error ranges in quadrature the total root mean square (RMS) for each range is between 0.2828″ and 1.1314″ for GSC I, and between 0.2828″ and 0.3960″ for GSC II. The Sloan Digital Sky Survey (SDSS) has an astrometric accuracy per coordinate of 0.10″ for average seeing and at the survey limit of $r \sim 22$ (Pier et al. 2003). When adding this RMS value in quadrature the result is 0.1414″.

Using the astrometric header keywords crval1, crval2, o_crval1, o_crval2, g_crval1, g_crval2, s_crval1, and s_crval2 , where 1 and 2 refer to right ascension and declination, respectively, we were able to determine if the absolute HST astrometry has been updated to external catalogues. Before stating how to determine if the astrometry has been updated providing a definition of the aforementioned header keywords is in order. As stated previously, 1 and 2 refers to either right ascension or declination, crval refers to the active astrometric zeropoint, o_crval refers to original astrometric zeropoint after drizzling and rotation to north-up but before an astrometric correction has been accomplished based on matching to GSC II and SDSS, g_crval and s_crval are the solution values after matching to GSC II and SDSS, respectively. The other astrometric header keywords incorporated in this analysis are: g_dra, g_ddec (right ascension and declination offset between HST and GSC II), g_rmsra, g_rmsdec (right ascension and declination RMS values of matched sources within GSC II), and g_nmatch (number of sources in GSC II). There are analogous header keywords for SDSS (s instead of g in the header keyword names). The test for determining whether the astrometry has been updated consists of comparing these header keywords with each other. This is done by looking at the absolute values of the differences between these various astrometric header keywords. For example, consider the differences between crval1, o_crval1, and g_crval1. If the absolute difference between crval1 and g_crval1 (crval1 - g_crval1) is less than the absolute difference between crval1 and o_crval1 (crval1 - o_crval1), and the same condition for the declination exists, then the HLA astrometry has been updated to GSC II in this particular example. This current analysis of the astrometric header keyword values uses datasets that have have been updated to GSC II and SDSS.

In addition to having been determined by updating to external catalogues the total offsets and RMSs were verified by visual inspection, particularly for the total RMS, of the drizzled image to see if the number of matches reported in the header keywords are valid. This lead to the classification of the datasets as “passed”, “failed” or “undecided”. Failures are defined when either Guide Star Catalogue II or Sloan Digital Sky Survey sources are over-plotted on Hubble Legacy Archive drizzled images and reveal no or few resulting matches. This is done by plotting circles on Hubble Space Telescope images where Guide Star Catalogue II and Sloan Digital Sky Survey sources should be according to their specific right ascension and declination but finding nothing in the circle or by erroneously encapsulating regions of extended sources. These “mis-matches” result in erroneous high total root mean square values which contaminate the extended tails of the histograms. There are numerous reasons for the mis-matches and correcting these reasons, if possible, will significantly mitigate these extended tails. On the other hand, if there are enough matches then the dataset is

designated as "passed". Furthermore, a dataset is classified as "undecided" when there is no means of determining whether the RMS or offset values are valid or not by visual inspection.

The format of this paper is: §2 is the investigation of histograms, §3 is the reasons for the mismatches found, §4 talks about the lack of the $\cos(\delta)$ scaling factor propagated in the right ascension, §5 provides conclusions, §6 has references, and §7 is an appendix which provides histograms and throughput curves used in the analysis but not presented in the main body of the paper.

2. Investigation of Histograms

2.1. Total Offsets Between HST, GSC I, GSC II, and SDSS

In this section an analysis of several histograms is presented, which are found in Figures 1, 2, 3, and 4. To begin look at Figures 1 and 2. These figures show a Gaussian fit to the histograms of astrometric information found in the final drizzled ACS images produced by HLA. Figure 1 shows astrometric data when HST uses GSC I for pointing accuracy and Figure 2 shows the same type of information but when HST employs GSC II for pointing accuracy. The center of the distributions derived from the Gaussian fits show markedly differing peaks. The reason for this behavior derives from the fact that the total absolute astrometric error of HST when using GSC I is larger than the total absolute astrometric error when using GSC II. The center of the distribution peaks are, as found in Figures 1 and 2, $0.7706''$ and $0.4677''$, respectively. Figures 3 and 4 show the same type of behavior, except that WFPC2 has been updated to SDSS. Here, as in Figure 1 and 2, the time stamp of the modified Julian date (MJD) delineates the boundary between when GSC I and GSC II were used for pointing accuracy. The value of the center of the distributions are $0.7473''$ when MJD < 53917.0 and $0.3270''$ when MJD ≥ 53917.0. Again notice the significantly disparate values of the peaks. Furthermore, ACS astrometric header information was updated to SDSS and WFPC2 was updated to GSC I and GSC II as well, but the histograms are not shown here but can be found in the Appendix. There are two columns of statistics in the legends of Figures 1, 2, 3, and 4 which describes the properties of the distribution itself (first column) and describes the properties of the Gaussian fit to the distribution (second column).

Tables 1 and 2 provide all of the information derived from fitting a Gaussian to various combinations among ACS, WFPC2, GSC I, GSC II, and SDSS. The columns for Tables 1 and 2 are: the first two present the detector and filters, the next two are the number of datasets that went into generating the histograms, and the next six contain various statistics derived from fitting Gaussian distributions to the histograms for GSC I, GSC II, and SDSS, respectively.

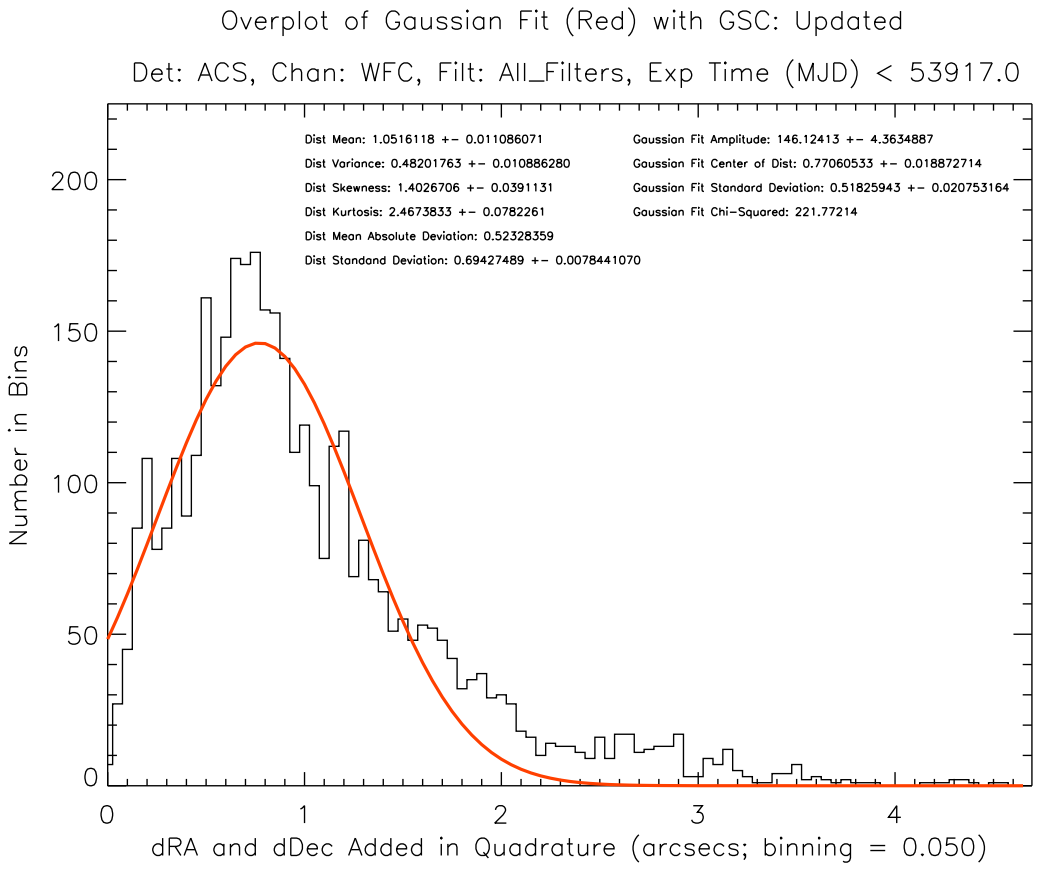

Fig. 1.— In this histogram the center of the Gaussian fit measurement is an attribute of the error inherent in HST absolute astrometry due to uncertainties in the positions of the guide stars. Note that the histogram is a plot of the total offset between HST and GSC I (MJD < 53917.0). The center of the Gaussian fit is $0.7706''$. There are two columns of statistics in the legend of this figure which describes the properties of the distribution itself (first column) and describes the properties of the Gaussian fit to the distribution (second column).

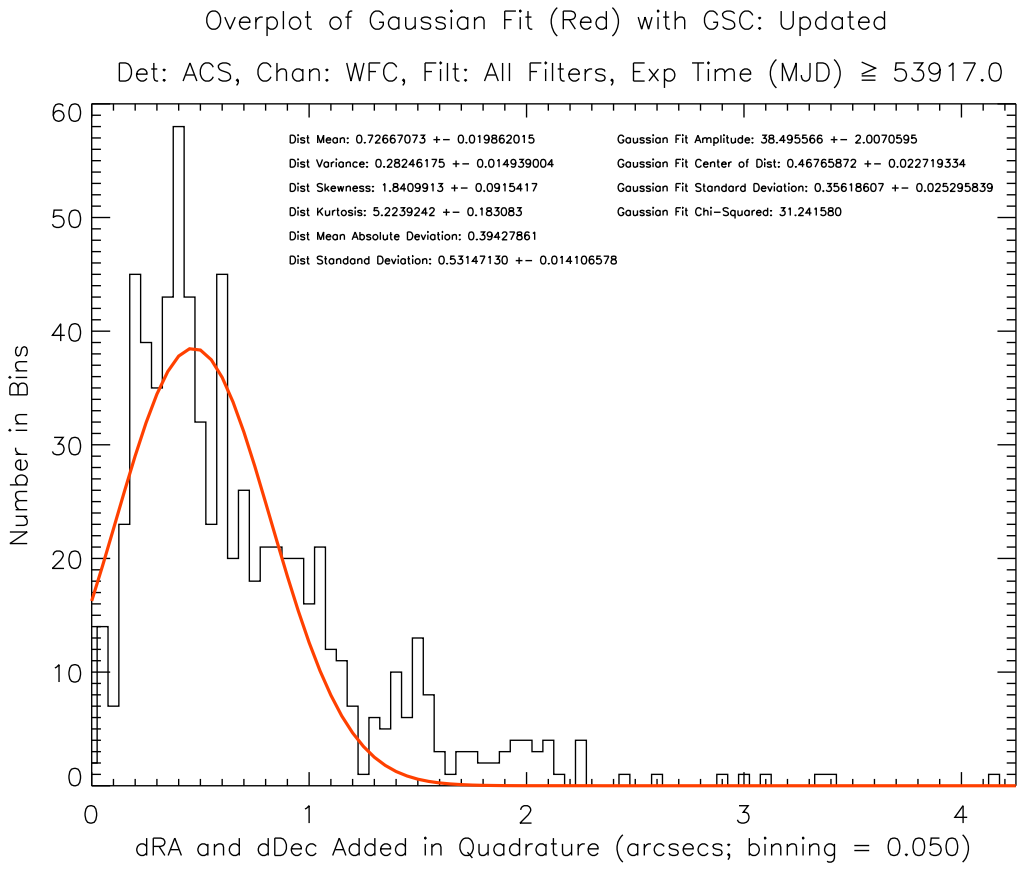

Fig. 2.— In this histogram the center of the Gaussian fit measurement is an attribute of the error inherent in HST absolute astrometry due to uncertainties in the positions of the guide stars. Note that the histogram is a plot of the total offset between HST and GSC II (MJD $\geq$ 53917.0). The center of the Gaussian fit is $0.4677''$. There are two columns of statistics in the legend of this figure which describes the properties of the distribution itself (first column) and describes the properties of the Gaussian fit to the distribution (second column).

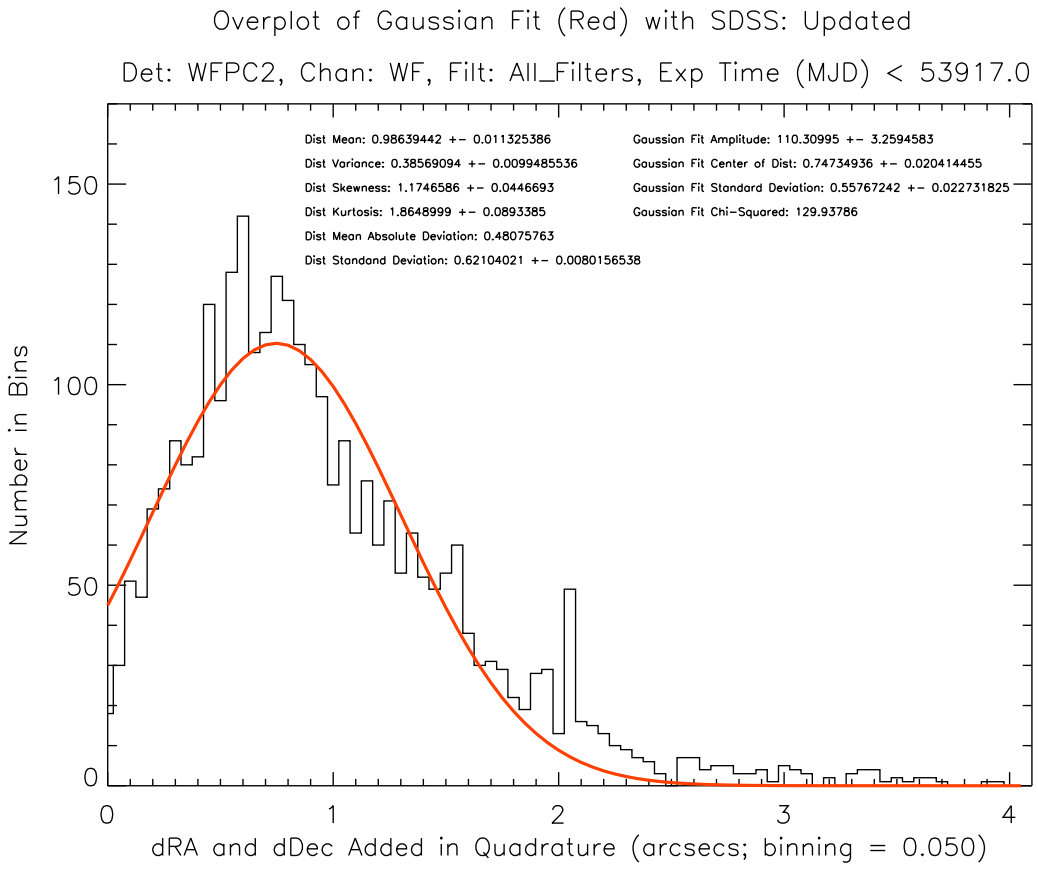

Fig. 3.— In this histogram the center of the Gaussian fit measurement is an attribute of the error inherent in HST absolute astrometry due to uncertainties in the positions of the guide stars. Note that the histogram is a plot of the total offset between HST and GSC I (MJD < 53917.0). The center of the Gaussian fit is $0.7473''$. There are two columns of statistics in the legend of this figure which describes the properties of the distribution itself (first column) and describes the properties of the Gaussian fit to the distribution (second column).

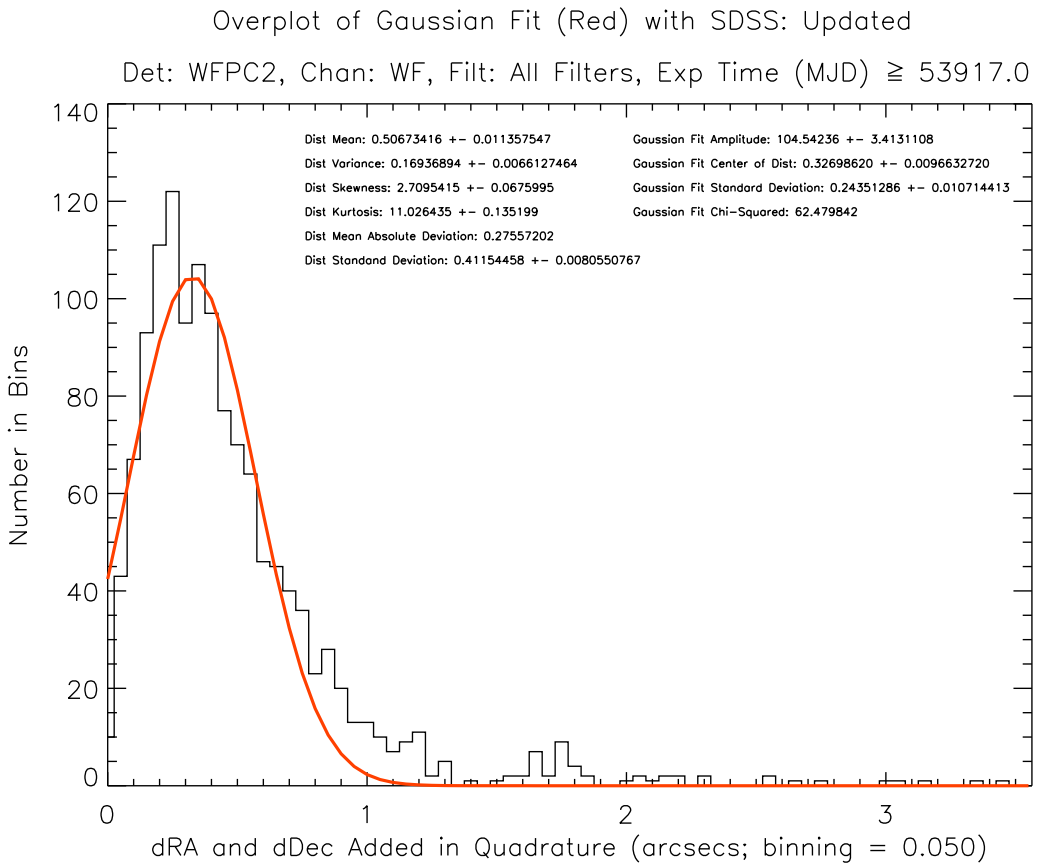

Fig. 4.— In this histogram the center of the Gaussian fit measurement is an attribute of the error inherent in HST absolute astrometry due to uncertainties in the positions of the guide stars. Note that the histogram is a plot of the total offset between HST and GSC II (MJD $\geq$ 53917.0). The center of the Gaussian fit is $0.3270''$. There are two columns of statistics in the legend of this figure which describes the properties of the distribution itself (first column) and describes the properties of the Gaussian fit to the distribution (second column).

Table 1: dRA and dDec Added in Quadrature: MJD $<$ 53917.0 (Gaussian Fit)

Detector	Filter	Number of Datasets		Center of Distribution		Standard Deviation		χ^2	
		GSC I	SDSS	GSC I	SDSS	GSC I	SDSS	GSC I	SDSS
ACS	All	3922	2339	0.7706 ± 0.01887	0.8257 ± 0.01638	0.5183	0.5185	221.7721	67.5301
WFPC2	All	6036	3007	0.7895 ± 0.01488	0.7473 ± 0.02041	0.5681	0.5577	246.0673	129.9379

Table 2: dRA and dDec Added in Quadrature : MJD $\geq$ 53917.0 (Gaussian Fit)

Detector	Filter	Number of Datasets		Center of Distribution		Standard Deviation		χ^2	
		GSC II	SDSS	GSC II	SDSS	GSC II	SDSS	GSC II	SDSS
ACS	All	716	448	0.4677 ± 0.02272	0.4238 ± 0.01930	0.3562	0.3551	31.2416	9.5619
WFPC2	All	1476	1313	0.4433 ± 0.01058	0.3270 ± 0.009663	0.3217	0.2435	36.3379	62.4798

The absolute astrometry for HST images have total typical errors between 0.2828″ and 1.1314″ for GSC I, between 0.2828″ and 0.3960″ for GSC II. Investigation of the "Center of Distribution" column in Table 1 shows that the total offset values fall within the ranges given for GSC I and Table 2 shows that the total offset values are greater than the upper limit for the range of values for GSC II and larger than the SDSS total RMS value. These values make sense in that it is unexpected for these total offset values to be less than the lower limit ranges for GSC I and GSC II and to be below the SDSS total RMS value. What is immediately obvious is the switch to the smaller total errors in GSC II that is reflected in the much smaller values of the total offsets for both GSC II and SDSS. The percentage difference between GSC I and GSC II total offsets is 41.6% and the differences in SDSS for differing GSCs is 52.3%. Note that the targeting accuracy of HST is directly linked to the GSCs so when the pointing accuracy was improved by using GSC II the total offset between HST and SDSS (and other external catalogues) improves as well.

2.2. Total RMSs Derived from the GSC II and SDSS Catalogs

Figures 5 and 6 show an overlay of GSC II and SDSS right ascension RMSs and declination RMSs that have been added in quadrature so that the histograms show the total RMS values for GSC II and SDSS. Inspection of Figures 5 and 6 show decidedly different distributions than those found in Figure 1, 2, 3, and 4. Figures 5 (ACS) and 6 (WFPC2) portray two different values for the peak of the histograms (GSC II in black and SDSS in red). The reason for this is that these RMS values are derived from the GSC II and SDSS catalogs themselves and are not internal to HST (therefore the MJD delineation can be neglected). Moreover, in Figure 5 the GSC II histogram shows an extended tail while for the SDSS histogram there are very little numbers in bins beyond 0.5″. Figure 6, on the other hand, shows the same information as Figure 5, but both GSC II and SDSS show extended tails that have significant numbers in bins up to 1.2″ after which the number in bins quickly taper to zero. The reason for number in bins, for both Figures 5 and 6, are due significantly to mis-matches discovered when over-plotting GSC II and SDSS sources on HLA combined drizzled images which are represented as open circles when overlayed on HLA combined drizzled images. These extended tails were somewhat mitigated by generating histograms that used individual filters and not a combination of all filters as was used to create Figures 5 and 6 (more figures of this type can be found in the Appendix). The various reasons for these mis-matches are explained in detail in §3.

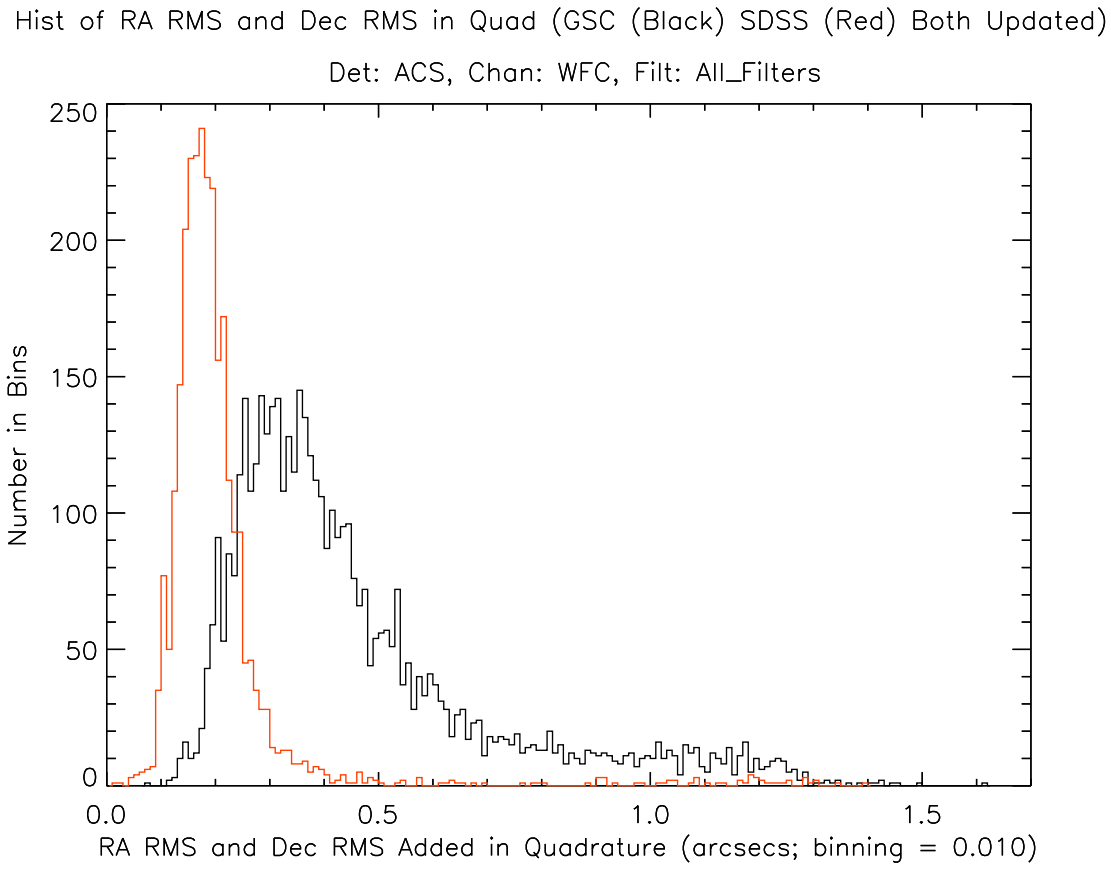

Fig. 5.— In this histogram both peaks do not have the approximate same value because RMS values are derived from the GSC II and the SDSS catalogues themselves. Since both catalogues have different RMS values this will be represented as differing peak values of the histograms. The peak for GSC II is $\approx 0.32''$ and the peak value for SDSS is $\approx 0.20''$. Note that the tail of the GSC II histogram (black) does not taper down to zero until about $1.2''$ after which the taper to zero proceeds quickly.

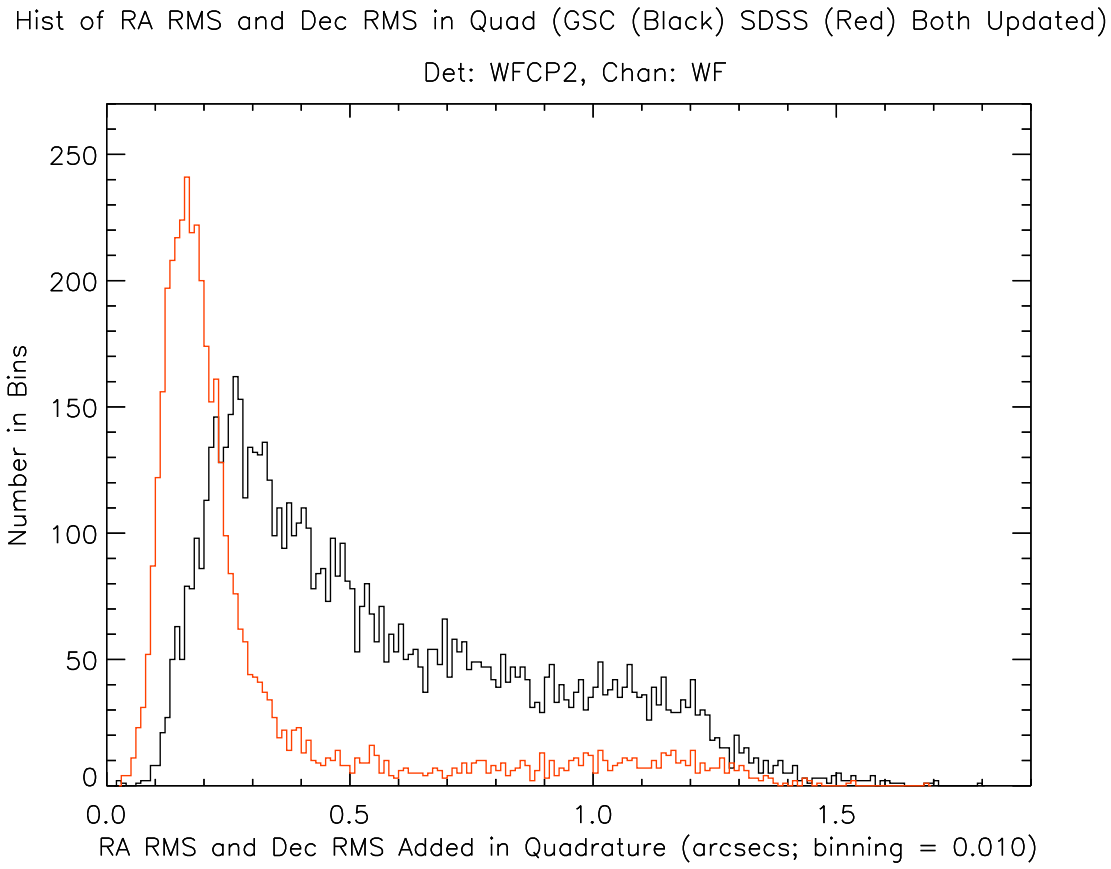

Fig. 6.— In this histogram both peaks do not have the approximate same value because RMS values are derived from the GSC II and the SDSS catalogs themselves. Since both catalogs have different RMS values this will be represented as differing peak values of the histograms. The peak for GSC II is $\approx 0.29''$ and the peak value for SDSS is $\approx 0.17''$. Note that the tail of the GSC II histogram (black) and the tail of the SDSS histogram (red) does not taper down to zero until about $1.2''$ after which the taper to zero proceeds quickly.

Table 3: RA RMS and Dec RMS Added in Quadrature (Gaussian Fit)

Detector	Filter	Number of Datasets		Center of Distribution		Standard Deviation		χ^2	
		GSC II	SDSS	GSC II	SDSS	GSC II	SDSS	GSC II	SDSS
ACS	All	7657	3202	0.3440 ± 0.003667	0.1718 ± 0.0006851	0.1213	0.04346	161.4072	53.3982
ACS	F435W	920	352	0.4295 ± 0.02117	0.2036 ± 0.005631	0.2305	0.06683	7.6620	2.7537
ACS	F475W	584	272	0.3816 ± 0.006132	0.1770 ± 0.002160	0.1320	0.04039	1.7352	1.7704
ACS	F555W	680	270	0.4668 ± 0.03590	0.1823 ± 0.002144	0.2750	0.04997	4.6757	1.3014
ACS	F606W	2001	718	0.3446 ± 0.005953	0.1734 ± 0.001669	0.1169	0.04997	32.7096	4.1436
ACS	F625W	352	83	0.2866 ± 0.01430	0.1537 ± 0.003204	0.1075	0.03539	4.0964	1.0159
ACS	F775W	2959	1048	0.2978 ± 0.005018	0.1685 ± 0.001157	0.1051	0.03710	19.1782	2.4076
ACS	F814W	3355	1849	0.3693 ± 0.003792	0.1653 ± 0.0007110	0.1156	0.03580	20.5821	21.1541

Table 4: RA RMS and Dec RMS Added in Quadrature (Gaussian Fit)

Detector	Filter	Number of Datasets		Center of Distribution		Standard Deviation		χ^2	
		GSC II	SDSS	GSC II	SDSS	GSC II	SDSS	GSC II	SDSS
WFPC2	All	28389	9754	0.4089 ± 0.01582	0.1676 ± 0.001200	0.3062	0.05890	549.8281	113.6601
WFPC2	F439W	1227	153	0.5842 ± 0.06610	0.1520 ± 0.009719	0.4865	0.07755	5.7755	1.9084
WFPC2	F450W	2303	891	0.3420 ± 0.01646	0.1640 ± 0.002683	0.2039	0.06463	29.6414	9.2415
WFPC2	F555W	3931	1106	0.4748 ± 0.02200	0.1352 ± 0.002816	0.3230	0.06603	18.4167	4.1601
WFPC2	F606W	11768	4104	0.3394 ± 0.007377	0.1626 ± 0.001068	0.1688	0.05320	27.1796	6.2354
WFPC2	F814W	8594	3235	0.3810 ± 0.009538	0.1709 ± 0.001270	0.2032	0.05749	35.5816	15.6332

As stated before, the absolute astrometry for HST images have total typical errors between $0.2828''$ and $0.3960''$ for GSC II, and $0.1414''$ for SDSS. Investigation of the "Center of Distribution" column in Table 3 shows that the total RMS values fall within the ranges and above the upper limit given for GSC II and above the SDSS total RMS value when using ACS. Table 4 also shows that the total RMS values are greater than the range of values for GSC II and larger than the SDSS total RMS value, except for one case involving F555W which is less than $0.1414''$ (difference of 4.38%). These values make sense (except one) in that it is unexpected for these total offset values to be less than the lower limit ranges for GSC II and to be below the SDSS total RMS value.

3. Reasons for Mis-matches

The extended tails found in Figures 5 and 6 were analyzed to see if matches could be determined by over-plotting GSC II and SDSS sources on HST combined drizzled images produced from the HLA pipeline. Several hundred datasets were examined by eye to determine if the matches were real or not (*i.e.*, mis-matches). Various reasons for mis-matches emerged from this analysis.

Mis-matches are defined when either GSC II or SDSS sources are over-plotted on HLA drizzled images with no or few resulting matches. This is done by plotting circles on HST images where GSC II and SDSS sources should be according to their specific right ascension and declination but finding nothing in the circle or by encapsulating erroneous regions of extended sources. There are numerous reasons for mis-matches and each reason found in the analysis will be explained. The list of reasons is as follows: Ultra-violet (UV) and Narrow Filter contamination, poor image combination, poor image combination due to moving target observations, all GSC II or SDSS circles being shifted, not enough matches and spurious detections, only 1 image present as in a MAST preview, not enough circles in the HST field of view (FOV), and datasets that are spectroscopic (grism data) and not photometric.

A description of each reason is presented hence:

1) HST UV and Narrow Filter contamination causes mis-matches because of the low throughput when compared to GSC II and SDSS throughputs. Figures 7 and 8 show the various throughput

curves of the photometric filters contributing to this analysis. Note especially the negligible or non-existent throughput for both GSC II (Figure 7) and SDSS (Figure 8) at 3000Å (see Appendix for two more throughput plots). For instance, if the combined drizzled image has only F300W images then when either GSC II or SDSS sources are over-plotted on the HST image the circles fall on blank regions resulting on no matches. Also, if the HST combined drizzled images contain UV filters then GSC II and SDSS sources can also fall on blank regions. The same low throughput logic applied to UV filters can also be applied to Narrow filters as well with the results being the same, namely that GSC II and SDSS sources over-plotted on the drizzled images fall on blank regions. Because of this type of mis-match histograms containing only information from individual filters were generated and then examined (see §2).

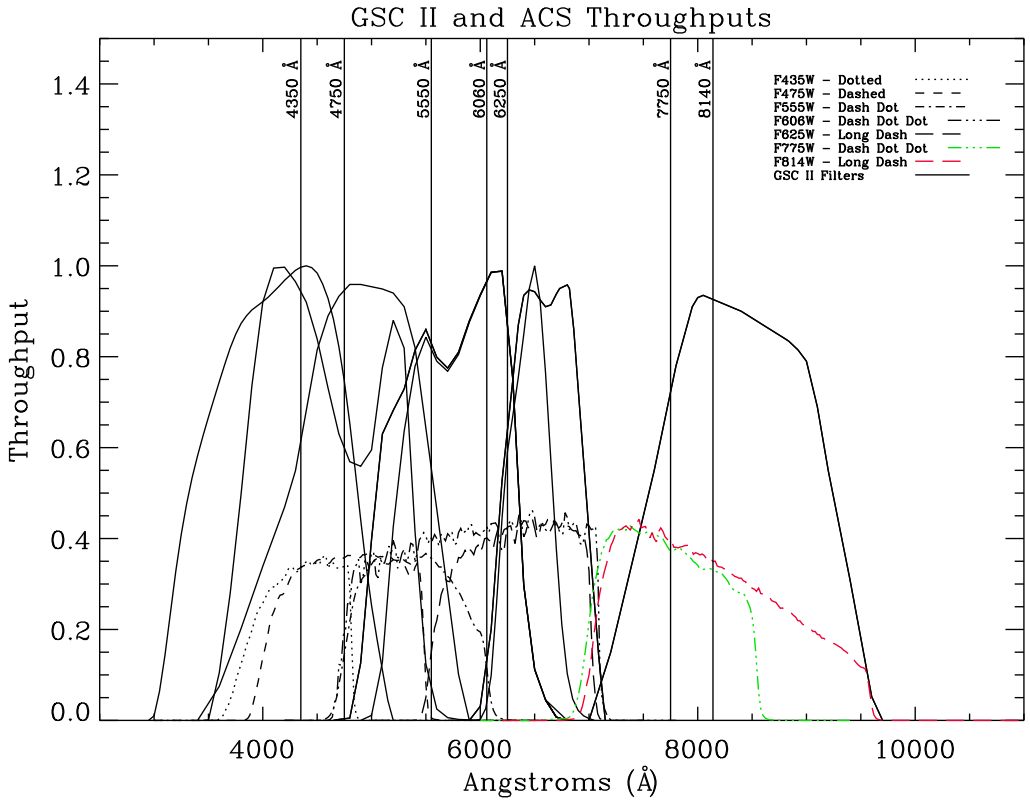

Fig. 7.— This figure portrays a comparison of GSC II and ACS throughput filter curves. The legend in the plot describes what each throughput curve represents. The vertical lines show the approximate effective wavelength.

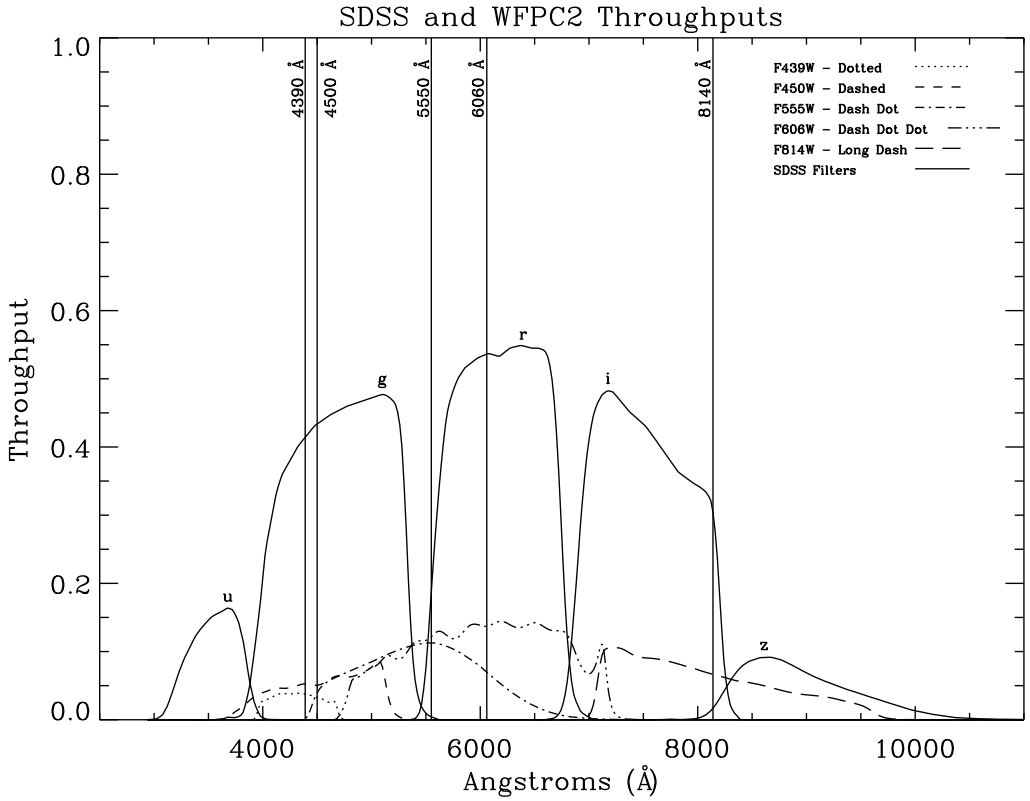

Fig. 8.— This figure portrays a comparison of SDSS and WFPC2 throughput filter curves. The legend in the plot describes what each throughput curve represents. The vertical lines show the approximate effective wavelength.

2) Poor image combination is when the HLA pipeline combines images that are not properly aligned for whatever reason. This results in GSC II and SDSS sources falling on blank regions or cosmic rays (CR) or image artifacts.

3) Moving target poor image combination happens when the HLA pipeline attempts to combine images of a moving target within the same visit. Because the target is not in the same place in the single images that become a combined drizzled image the alignment can be poorly done. As a result GSC II and SDSS circles can identify blank regions, CR, and/or image artifacts.

4) The mis-match reason shifted means that all of the sources in GSC II and SDSS are all offset from image sources in the same direction and by the same amount. This could be the effect of a minus sign being applied inappropriately.

5) Not enough matches and spurious detections means that some of the GSC II and SDSS sources have been identified in the combined drizzled images but not enough to coincide with the header keyword values of g_nmatch and s_nmatch. Furthermore, there are GSC II and SDSS sources that fall on blank regions identifying them as spurious detections.

6) Sometimes when overplotting GSC II and SDSS sources, within the HLA, a MAST preview

image is all that is available for certain datasets and since this is a single image the HST FOV will be contaminated with CR, hot and warm pixels, and image artifacts. This will cause some of the GSC II and SDSS sources to be mis-identified as CR, hot and warm pixels, and have portions of image artifacts identified as GSC II and SDSS sources.

7) A rarer reason for mis-matches results from when there are not enough GSC II and SDSS circles in the HST FOV but are mostly in the surrounding halo of GSC II and SDSS FOVs. In other words the GSC II and SDSS sources within the HST FOV do not match the numbers provided by the header keywords g_nmatch and s_nmatch.

8) Another rare reason for a failure is that in 3 datasets chosen from the extended tails of a histogram using individual filters there were no corresponding images of the prescribed individual filters in the HLA (filters F555W and F606W; see Tables 20 and 21).

9) One dataset turned out to be a grism observation and not a photometric observation.

Tables 5 to 22 house the various reasons for the mis-matches discovered. To start Tables 5 to 10 have mis-match reasons when all of the available filters for ACS and WFPC2 were used to generate the total RMS histograms. Moreover, Tables 11 to 22 have mis-match reasons when using individual ACS and WFPC2 filters. The most notable difference between these two scenarios is that there is no UV and Narrow filter contamination for mis-matches when considering the individual filter examinations for obvious reasons.

For Tables 5 to 22 the first row designates the detector and which filter was used or if all of the filters were used, after the first row come three columns in which the first column houses the reason for the mis-match, the second and third columns pertain to how many times the reason was invoked to explain a mis-match. After the columns in each table there is a row with the range of total RMS values, as determined by examination of histograms of the all and individual filter type, in which numerous datasets were visually examined in HLA to determine if the RMS values are true or not. In some instances the RMS range is not the same for GSC II and SDSS and so another row was added after the first. The last row in each table contains the number of datasets visually inspected and the number of failures and passes for each external catalog. Additionally, especially with the individual filter cases, the amount of datasets used were different because the extended tails contained either more or less datasets (see Figures 7 and 8 for examples). Note that if a dataset had enough matches then that particular dataset "passed" and the RMS value could be trusted, if there were no or not enough matches then the RMS value was not trusted and was designated as "failed". Furthermore, datasets were also designated as "undecided" if the final drizzled image was unavailable through the public HLA website and as such there was no information to determine whether the dataset either "passed" or "failed".

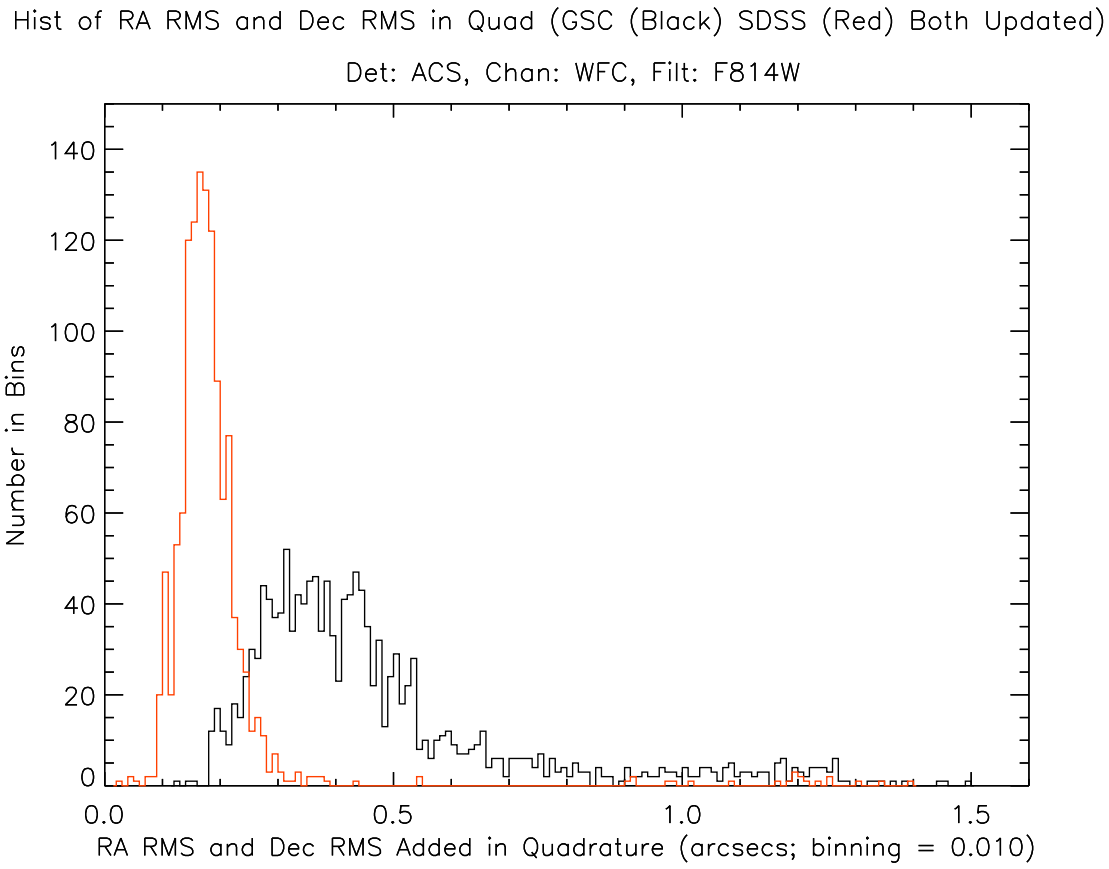

Fig. 9.— This figure is used to exemplify why the total RMS ranges can be different for different filters. Note the damped extended tail for SDSS when compared to GSC II.

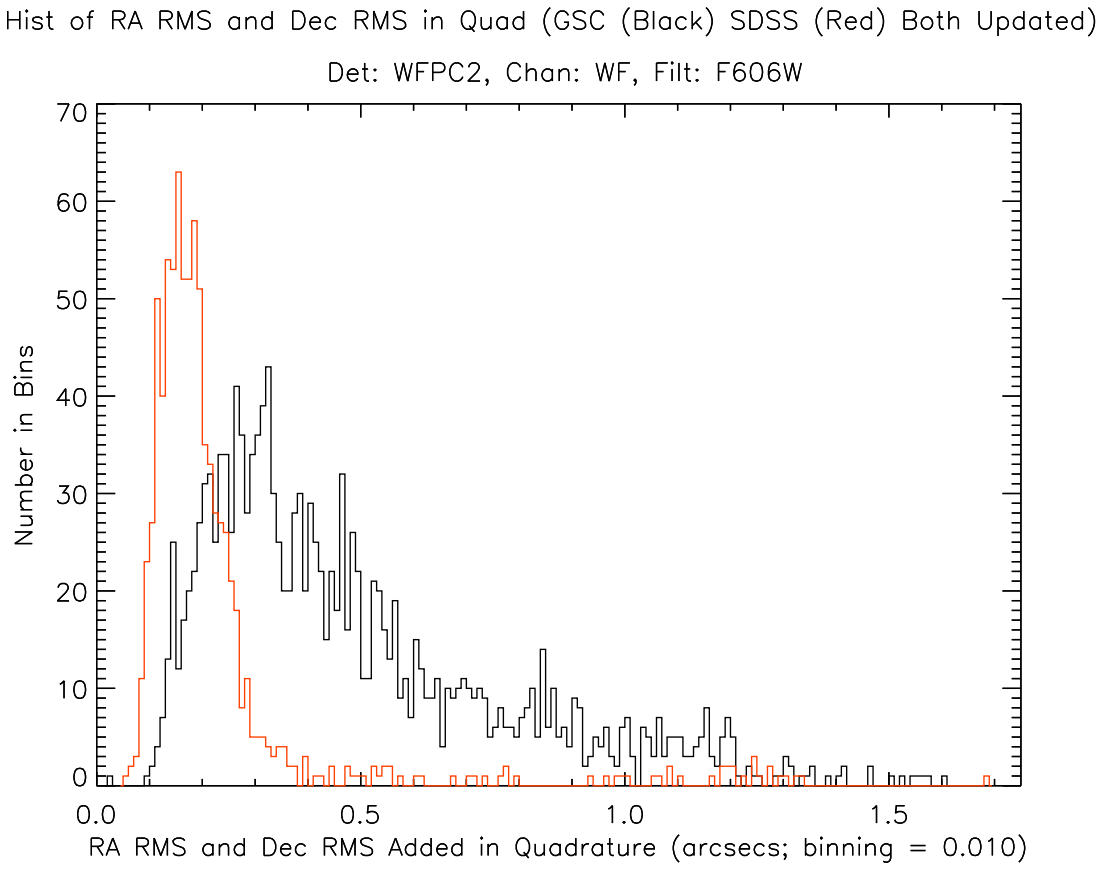

Fig. 10.— This figure is used to exemplify why the total RMS ranges can be different for different filters. Note the damped extended tail for SDSS when compared to GSC II.

3.1. All Filters Combined

This sub-section contains the tables in which all of the filters were used to create the total RMS histograms. Note that not all of the reasons for the mis-matches are in each table.

Table 5: Catagorization of Reasons for Mis-matches (ACS)

Mis-matches ACS All Filters		
Reason	GSC II	SDSS
Narrow Filters	1	-
Poor Image Combination	1	1
MT/Poor Image Combination	-	1
Shifted	4	1
Not Enough Matches/Spurious Detections	15	-
MAST Preview/1 image/CR	1	1
Grism	-	1
0.90 < total RMS < 1.10 (GSC II and SDSS)		
GSC II Total: 22, Fail: 21, Pass: 0, Undecided: 1, SDSS Total: 5, Fail: 4, Pass: 0, Undecided: 1		

Table 6: Catagorization of Reasons for Mis-matches (WFPC2)

Mis-matches WFPC2 All Filters		
Reason	GSC II	SDSS
UV Filters	11	11
Narrow Filters	-	2
Poor Image Combination	1	2
Shifted	-	3
Not Enough Matches/Spurious Detections	7	5
0.90 < total RMS < 1.10 (GSC II and SDSS)		
GSC II Total: 20, Fail: 19, Pass: 1, SDSS Total: 23, Fail: 22, Pass: 1		

Table 7: Catagorization of Reasons for Mis-matches (ACS)

Mis-matches ACS All Filters		
Reason	GSC II	SDSS
Narrow Filters	1	-
Poor Image Combination	1	-
MT/Poor Image Combination	-	1
Shifted	-	3
Not Enough Matches/Spurious Detections	1	-
MAST Preview/1 image/CR	1	-
1.20 < total RMS < 1.65 (GSC II and SDSS)		
GSC II Total: 4, Fail: 3, Pass: 0, Undecided: 1, SDSS Total: 4, Fail: 4, Pass: 0		

Table 8: Catagorization of Reasons for Mis-matches (WFPC2)

Mis-matches WFPC2 All Filters		
Reason	GSC II	SDSS
UV Filters	2	1
Narrow Filters	1	-
Poor Image Combination	-	1
MT/Poor Image Combination	3	1
Shifted	2	-
Not Enough Matches/Spurious Detections	1	1
MAST Preview/1 image/CR	1	-
1.30 < total RMS < 1.80 (GSC II and SDSS)		
GSC II Total: 10, Fail: 9, Pass: 0, Undecided: 1, SDSS Total: 4, Fail: 4, Pass: 0		

Table 9: Catagorization of Reasons for Mis-matches (ACS)

Mis-matches ACS All Filters		
Reason	GSC II	SDSS
Narrow Filters	-	1
Poor Image Combination	4	1
Shifted	-	1
Not Enough Matches/Spurious Detections	15	-
0.50 < total RMS < 0.80 (GSC II and SDSS)		
GSC II Total: 21, Fail: 19, Pass: 2, SDSS Total: 3, Fail: 3, Pass: 0		

Table 10: Catagorization of Reasons for Mis-matches (WFPC2)

Mis-matches WFPC2 All Filters		
Reason	GSC II	SDSS
UV Filters	1	7
Narrow Filters	1	2
Poor Image Combination	1	2
Not Enough Matches/Spurious Detections	8	2
0.50 < total RMS < 0.80 (GSC II and SDSS)		
GSC II Total: 21, Fail: 11, Pass: 10, SDSS Total: 21, Fail: 12, Pass: 9		

Not only were the datasets in the tail of the histogram inspected but datasets around the tallest peak in the histogram were analyzed as well. Four datasets, one at each end and two in the middle of the total RMS range were inspected and all four passed. The total RMS ranges analyzed are: WFPC2 0.25 < total RMS < 0.35 (GSC II) and 0.10 < total RMS < 0.20 (SDSS) and for

ACS 0.30 < total RMS < 0.40 (GSC II) and 0.10 < total RMS < 0.20 (SDSS).

3.2. Individual Filters: ACS

This sub-section contains the tables in which individual ACS filters were used to create the total RMS histograms. These filters are: F435W, F475W, F555W, F606W, F625W, F775W, and F814W. Note that not all of the reasons for the mis-matches are in each table.

Table 11: Catagorization of Reasons for Mis-matches

Mis-matches ACS F435W		
Reason	GSC II	SDSS
Not Enough Matches/Spurious Detections	9	-
0 matches, less than 10 circles in FOV	1	-
0.90 < total RMS < 1.30 (GSC II)		
0.25 < total RMS < 0.40 (SDSS)		
GSC II Total: 10, Fail: 10, Pass: 0, SDSS Total: 4, Fail: 0, Pass: 4		

Table 12: Catagorization of Reasons for Mis-matches

Mis-matches ACS F475W		
Reason	GSC II	SDSS
Shifted	-	2
Not Enough Matches/Spurious Detections	3	-
5 matches, less than 85 circles in FOV	1	-
0.90 < total RMS < 1.30 (GSC II)		
0.90 < total RMS < 1.40 (SDSS)		
GSC II Total: 4, Fail: 4, Pass: 0, SDSS Total: 2, Fail: 2, Pass: 0		

Table 13: Catagorization of Reasons for Mis-matches

Mis-matches ACS F555W		
Reason	GSC II	SDSS
Not Enough Matches/Spurious Detections	5	-
1 match, less than 20 circles in HST FOV	1	-
0.90 < total RMS < 1.30 (GSC II)		
0.25 < total RMS < 0.30 (SDSS)		
GSC II Total: 6, Fail: 6, Pass: 0, SDSS Total: 2, Fail: 0, Pass: 2		

Table 14: Catagorization of Reasons for Mis-matches

Mis-matches ACS F606W		
Reason	GSC II	SDSS
Poor Image Combination	-	1
MT/Poor Image Combination	-	2
Shifted	-	1
Not Enough Matches/Spurious Detections	8	-
MAST Preview/1 image/CR	1	-
0.90 < total RMS < 1.60 (GSC II)		
0.90 < total RMS < 1.40 (SDSS)		
GSC II Total: 10, Fail: 8, Pass: 1, Undecided: 1, SDSS Total: 5, Fail: 4, Pass: 1		

Table 15: Catagorization of Reasons for Mis-matches

Mis-matches ACS F625W		
Reason	GSC II	SDSS
Poor Image Combination	1	-
Shifted	1	-
Not Enough Matches/Spurious Detections	4	-
0.90 < total RMS < 1.30 (GSC II)		
0.25 < total RMS < 0.45 (SDSS)		
GSC II Total: 6, Fail: 6, Pass: 0, SDSS Total: 2, Fail: 0, Pass: 2		

Table 16: Catagorization of Reasons for Mis-matches

Mis-matches ACS F775W		
Reason	GSC II	SDSS
Shifted	2	1
Not Enough Matches/Spurious Detections	4	-
0.90 < total RMS < 1.30 (GSC II)		
0.90 < total RMS < 1.20 (SDSS)		
GSC II Total: 6, Fail: 6, Pass: 0, SDSS Total:1, Fail: 1, Pass: 0		

Table 17: Catagorization of Reasons for Mis-matches

Mis-matches ACS F814W		
Reason	GSC II	SDSS
Poor Image Combination	-	3
Shifted	-	3
Not Enough Matches/Spurious Detections	8	-
MAST Preview/1 image/CR	-	1
0.90 < total RMS < 1.55 (GSC II)		
0.90 < total RMS < 1.40 (SDSS)		
GSC II Total: 10, Fail: 10, Pass: 0, SDSS Total: 7, Fail: 6, Pass: 0, Undecided: 1		

3.3. Individual Filters: WFPC2

This sub-section contains the tables in which individual WFPC2 filters were used to create the total RMS histograms. These filters are: F439W, F450W, F555W, F606W, and F814W. Note that not all of the reasons for the mis-matches are in each table.

Table 18: Catagorization of Reasons for Mis-matches

Mis-matches WFPC2 F439W		
Reason	GSC II	SDSS
MT/Poor Image Combination	2	2
Shifted	2	1
Not Enough Matches/Spurious Detections	6	-
MAST Preview/1 image/CR	-	1
0.90 < total RMS < 1.60 (GSC II)		
0.90 < total RMS < 1.40 (SDSS)		
GSC II Total: 10, Fail: 10, Pass: 0, SDSS Total: 4, Fail: 3, Pass: 0, Undecided: 1		

Table 19: Catagorization of Reasons for Mis-matches

Mis-matches WFPC2 F450W		
Reason	GSC II	SDSS
MT/Poor Image Combination	1	-
Shifted	1	-
Not Enough Matches/Spurious Detections	4	1
MAST Preview/1 image/CR	1	2
1 image/CR/Streaks	1	-
0.90 < total RMS < 1.50 (GSC II)		
0.90 < total RMS < 1.40 (SDSS)		
GSC II Total: 8, Fail: 8 Pass: 0, SDSS Total: 3, Fail: 1, Pass: 0, Undecided: 2		

Table 20: Catagorization of Reasons for Mis-matches

Mis-matches WFPC2 F555W		
Reason	GSC II	SDSS
MT/Poor Image Combination	-	1
Shifted	-	2
Not Enough Matches/Spurious Detections	6	3
MAST Preview/1 image/CR	-	1
No F555W Filter	2	-
0.90 < total RMS < 1.60 (GSC II and SDSS)		
GSC II Total: 10, Fail: 6 Pass: 2, Undecided: 2, SDSS Total: 7, Fail: 6, Pass: 0, Undecided: 1		

Table 21: Catagorization of Reasons for Mis-matches

Mis-matches WFPC2 F606W		
Reason	GSC II	SDSS
Poor Image Combination	2	1
MT/Poor Image Combination	-	1
Shifted	2	2
Not Enough Matches/Spurious Detections	2	-
MAST Preview/1 image/CR	1	3
No F606W Filter	1	-
0.90 < total RMS < 1.70 (GSC II and SDSS)		
GSC II Total: 10, Fail: 6, Pass: 2, Undecided: 2, SDSS Total: 10, Fail: 4, Pass: 3, Undecided: 3		

Table 22: Catagorization of Reasons for Mis-matches

Mis-matches WFPC2 F814W		
Reason	GSC II	SDSS
Poor Image Combination	2	1
Shifted	1	1
Not Enough Matches/Spurious Detections	2	2
MAST Preview/1 image/CR	2	4
0.90 < total RMS < 1.60 (GSC II)		
0.90 < total RMS < 1.40 (SDSS)		
GSC II Total: 10, Fail: 5, Pass: 3, Undecided: 2, SDSS Total: 10, Fail: 4, Pass: 2, Undecided: 4		

3.4. Accumulated Mis-match Numbers

In this sub-section Tables 23 to 26 contain sums for each reason pertaining to a combination of all filters and individual filters for GSC II and SDSS. Tables 23 to 26 are structured this way: the first row contains filter and detector information, immediately below are three columns which house the reason for the mis-match in the first column and cumulated numbers for each mis-match reason for GSC II and SDSS, respectively. Table 27 is formatted as follows: the first row states that all of the datasets for both ACS and WFPC2 were combined for the numerical information found in the three succeeding columns. The first column states the meaning of the numbers found in the next two columns and the next two columns are the results for GSC II and SDSS, respectively.

Table 23: Number of Reasons for Mis-matches

All Filters ACS		
Reason	Number for GSC II	Number for SDSS
Narrow Filters	2	1
Poor Image Combination	6	2
MT/Poor Image Combination	-	2
Shifted	4	5
Not Enough Matches/Spurious Detections	31	-
MAST Preview/1 image/CR	2	1

Table 24: Number of Reasons for Mis-matches

All Filters WFPC2		
Reason	Number for GSC II	Number for SDSS
UV Filters	14	19
Narrow Filters	2	4
Poor Image Combination	2	5
MT/Poor Image Combination	3	1
Shifted	2	3
Not Enough Matches/Spurious Detections	16	8
MAST Preview/1 image/CR	1	-

Table 25: Number of Reasons for Mis-matches

Individual Filters ACS		
Reason	Number for GSC II	Number for SDSS
Poor Image Combination	1	4
MT/Poor Image Combination	-	2
Shifted	3	7
Not Enough Matches/Spurious Detections	41	-
MAST Preview/1 image/CR	4	1
0 matches, less than 10 circles in HST FOV	1	-
5 matches, less than 85 circles in HST FOV	1	-
1 match, less than 20 circles in HST FOV	1	-

Table 26: Number of Reasons for Mis-matches

Individual Filters WFPC2		
Reason	Number for GSC II	Number for SDSS
Poor Image Combination	4	3
MT/Poor Image Combination	3	4
Shifted	6	6
Not Enough Matches/Spurious Detections	20	6
MAST Preview/1 image/CR	4	11
1 image/CR/streaks	1	-
No F555W Filter	2	-
No F606W Filter	1	-

Table 27: Total Number of Datasets Analyzed

All and Individual Filters for Both WFPC2 and ACS		
Total Datasets Inspected	Number for GSC II	Number for SDSS
Total Number of Datasets	200	136
Fail	164	81
Pass	21	42
Undecided	15	13
Percentage Fail	82.0%	59.6%
Percentage Pass	10.5%	30.9%
Percentage Undecided	7.5%	9.5%

Table 27 provides the answer as to what is going on in the extended histogram tails. To begin a total of 336 datasets were visually examined and then classified as either passing, failing or undecided for the various reasons described in §3. Now combining the number of failed, passed, and undecided datasets for both GSC II and SDSS together the total failures are 245 datasets, total passed are 63 datasets, and total undecided datasets are 28. Converting these values to percentages the failure percentage is 72.9%, the pass percentage is 18.8%, and the undecided percentage is 8.3%. It is also interesting to note that when considering GSC II and SDSS separately the percentages (and numbers, see Table 27) change dramatically. For instance, the number of failures for GSC II is 164, the number of passes is 21, and the number of undecideds is 15 (total number of datasets is 200), which reflect a 82.0% failure rate, a 10.5% passing rate, and a 7.5% undecided rate. Doing the same thing for SDSS it is noted that the number of failures is 81, number of passes is 42, and number of undecideds is 13 (total number of datasets is 136), which convert to a 59.6% failure rate, a 30.9% passing rate, and a 9.5% undecided rate. Furthermore, there is a caveat and this is that the numbers quoted here cover all the total RMS ranges examined (see bottom rows Tables 1 to 18) so there are ranges (near and at the tallest peaks of the histograms) were it is expected that most if not all of the datasets will pass. As a result the extended tails will be effected more by the dataset failures than near the center of the histogram distribution. So what this means, for both GSC II and SDSS, is that the height of the extended tails (see Figures 1, 2, 3, 4, 5, 6, 9, and 10) can be explained as contamination from incorrect total RMS values due to mis-matches. If these were removed the extended tails would taper to zero at lower total RMS values. Additionally, if the failures that occur near the center of the distribution were removed then the standard deviations will be smaller and the extended tails will be shorter.

4. Scale Factor: $\cos(\delta)$

During this analysis large right ascension offsets (dRA) values were found ($46.4491''$ and $109.5458''$ for instance) which raised the question as to whether the dRA header values have been scaled by $\cos(\delta)$. Furthermore, the pointing errors of HST are far less than the aforementioned

values so there is no reason that there should be such large dRA values. Table 28 emphasizes how much difference is introduced when the $\cos(\delta)$ scale factor is neglected. The columns of Table 28 are: instrument, external catalog, proposal identification, visit, declination, unscaled dRA, and scaled dRA. Notice especially the entries for when WFPC2 and ACS are compared to GSC II.

Table 28: Scale Factor: $\cos(\delta)$

Instrument	Catalog	Proposal ID	Visit	Declination (δ)	Unscaled dRA	Scaled dRA ($\cos(\delta)$)
WFPC2	GSC II	9709	t0	89.2621°	46.4491″	0.5595″
WFPC2	SDSS	9710	oq	62.3999°	6.9382″	3.2145″
ACS	GSC II	9984	ni	89.3305°	109.5458″	1.2800″
ACS	SDSS	9575	cb	62.2880°	6.0727″	2.8240″

5. Conclusions

As shown by comparing the values in the "Center of Distribution" column in Tables 1 and 2 the total offset values fall within the total RMS ranges given for GSC I and GSC II and exceed the total RMS value given for SDSS. This behavior is what is expected. Furthermore and immediately obvious, is the switch to the smaller total errors in GSC II that is reflected in the much smaller values of the total offsets for both GSC II and SDSS. The percentage difference between GSC I and GSC II total offsets is 41.6% and the differences in SDSS for differing GSCs is 52.3%. Note that the targeting accuracy of HST is directly linked to the GSCs so when the pointing accuracy was improved by using GSC II the total offset between HST and SDSS (and other external catalogues) improves as well.

Investigation of the "Center of Distribution" columns in Table 3 and 4 show that the total RMS values fall within the ranges and above the upper limit given for GSC II and above the SDSS total RMS value for both ACS and WFPC2, except for one case involving F555W which is 0.1352″ as opposed to 0.1414″ and is a 4.38% difference. For the majority of values this is expected behavior.

Section 3 provides the answer as to what is going on in the extended histogram tails. A total of 336 datasets were visually examined and then classified as either passing, failing or undecided for the various reasons described in §3. Now combining the number of failed, passed or undecided datasets for both GSC II and SDSS together the total failures are 245 datasets, total passed are 63 datasets, and total undecided datasets are 28. Furthermore, there is a caveat and this is that the numbers quoted here cover all of the total RMS ranges examined so there are ranges, near and at the tallest peaks of the histograms, where it is expected that most if not all of the datasets will pass. As a result the extended tails will be effected more by the dataset failures than near the center of the histogram distribution. So what this means, for both GSC II and SDSS, is that the height of the extended tails can be explained as contamination from incorrect total RMS values due to mis-matches. If these were removed the extended tails would taper to zero at lower total

RMS values.

6. References

Lasker, B. M., et al. 2008, AJ, 136, 735
Pier, J. R., et al. 2003, AJ, 125, 1559
Russell, J. L., et al. 1990, AJ, 99, 2059

7. Appendix

The appendix contains plots used in astrometric analysis but not presented in the main body of this paper.

7.1. ACS: Plot of a Gaussian Fit to the Total RMSs Derived from GSC II

In the subsequent histograms the peaks have RMS values which are derived from GSC II. There are two columns of statistics in the legends of the subsequent figures which describes the properties of the distribution itself (first column) and describes the properties of the Gaussian fit to the distribution (second column). The total RMS range is between 0.2828″ and 0.3960″ for GSC II.

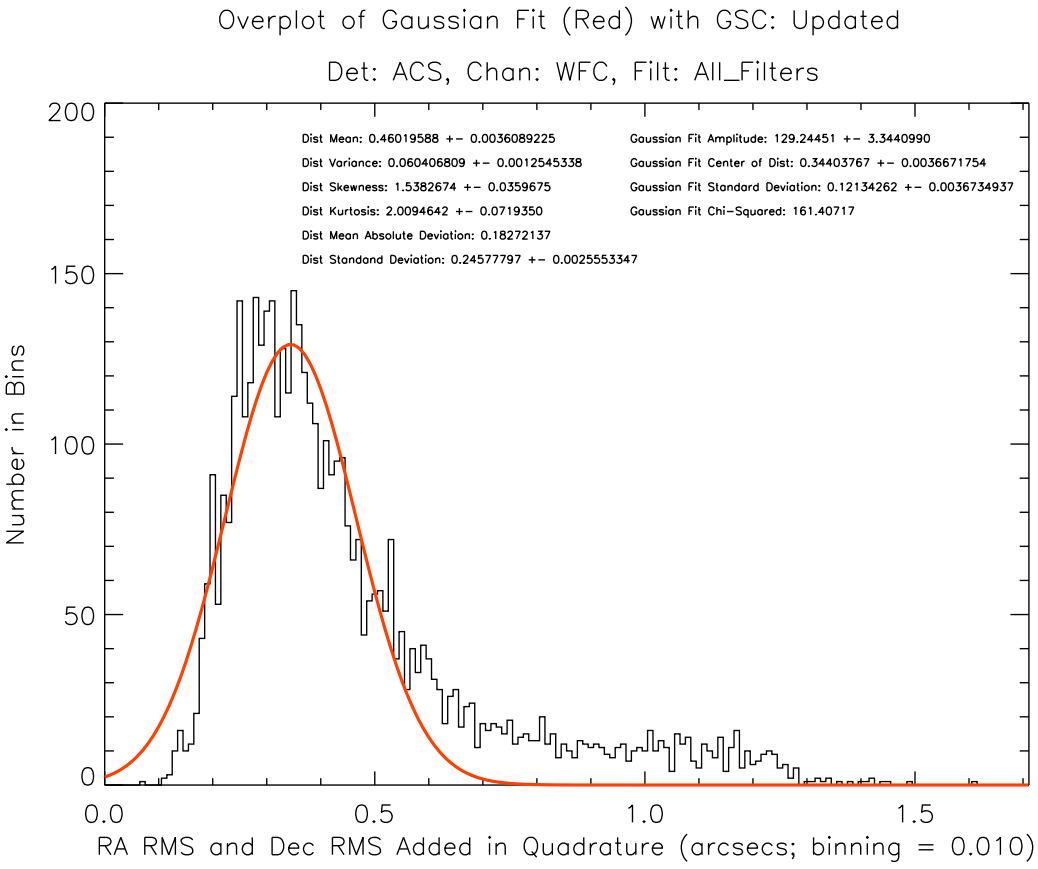

Fig. 11.— This plot shows the right ascension and declination RMSs added in quadrature. All filters were used to make this histogram.

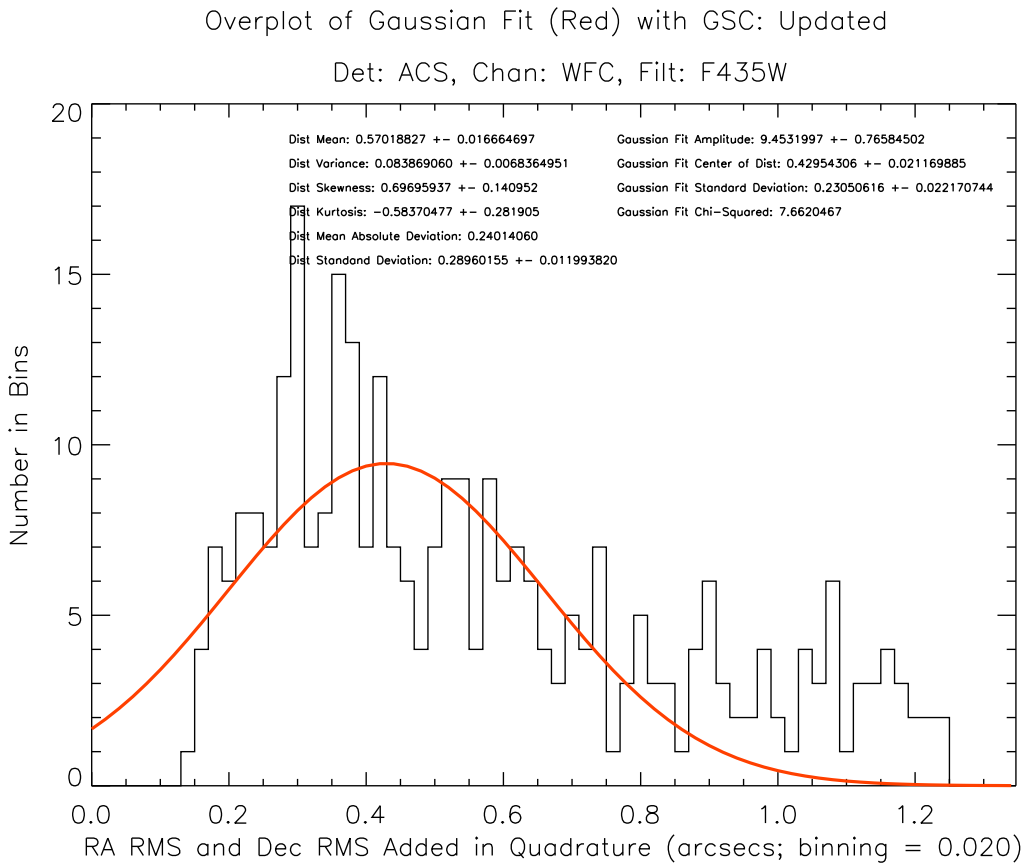

Fig. 12.— This plot shows the right ascension and declination RMSs added in quadrature. F435W was used to make this histogram.

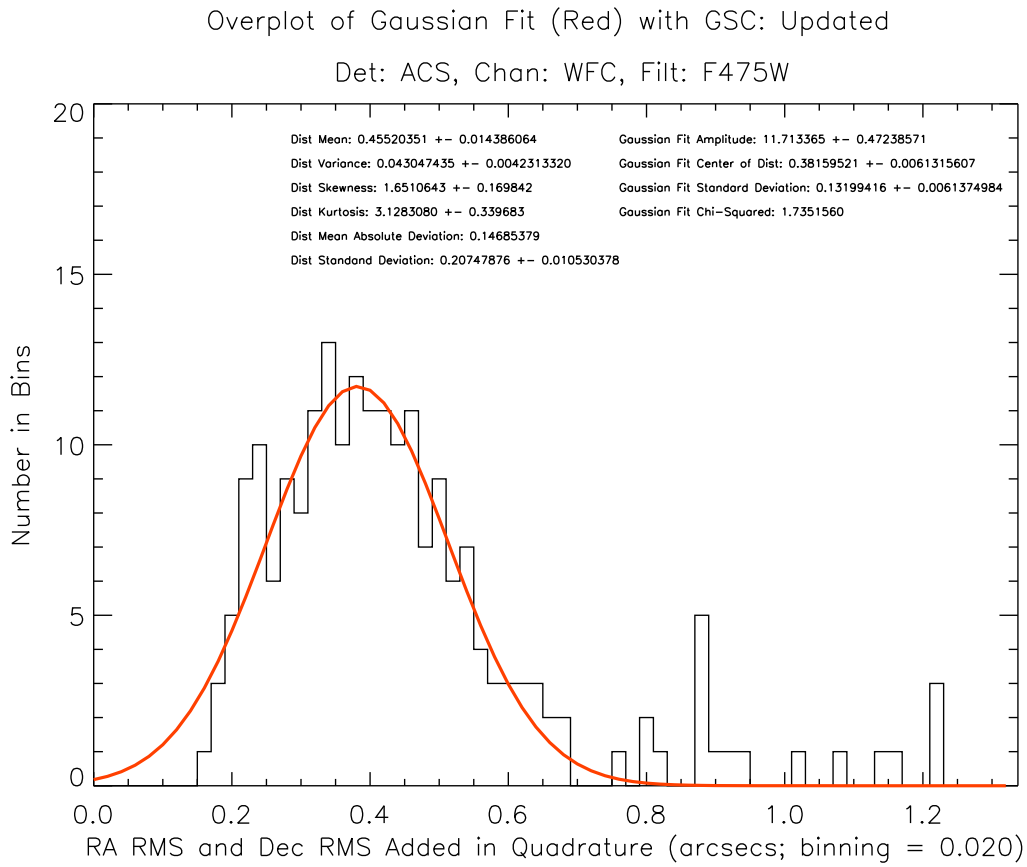

Fig. 13.— This plot shows the right ascension and declination RMSs added in quadrature. F475W was used to make this histogram.

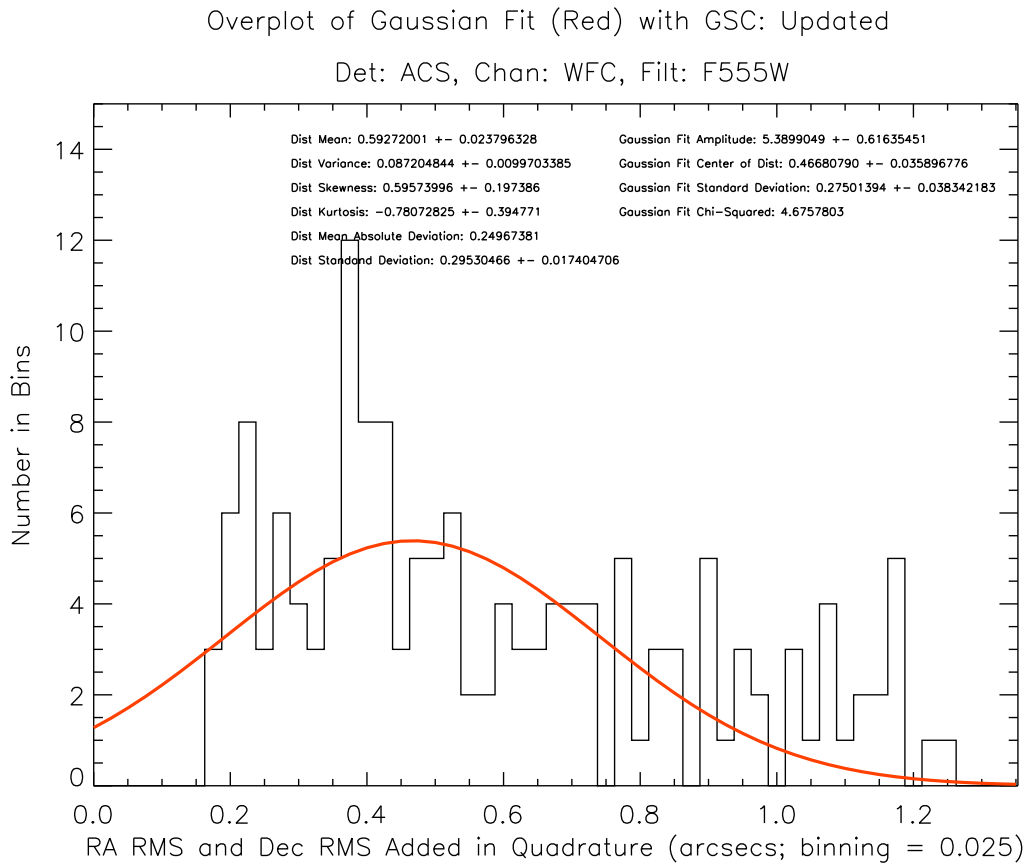

Fig. 14.— This plot shows the right ascension and declination RMSs added in quadrature. F555W was used to make this histogram.

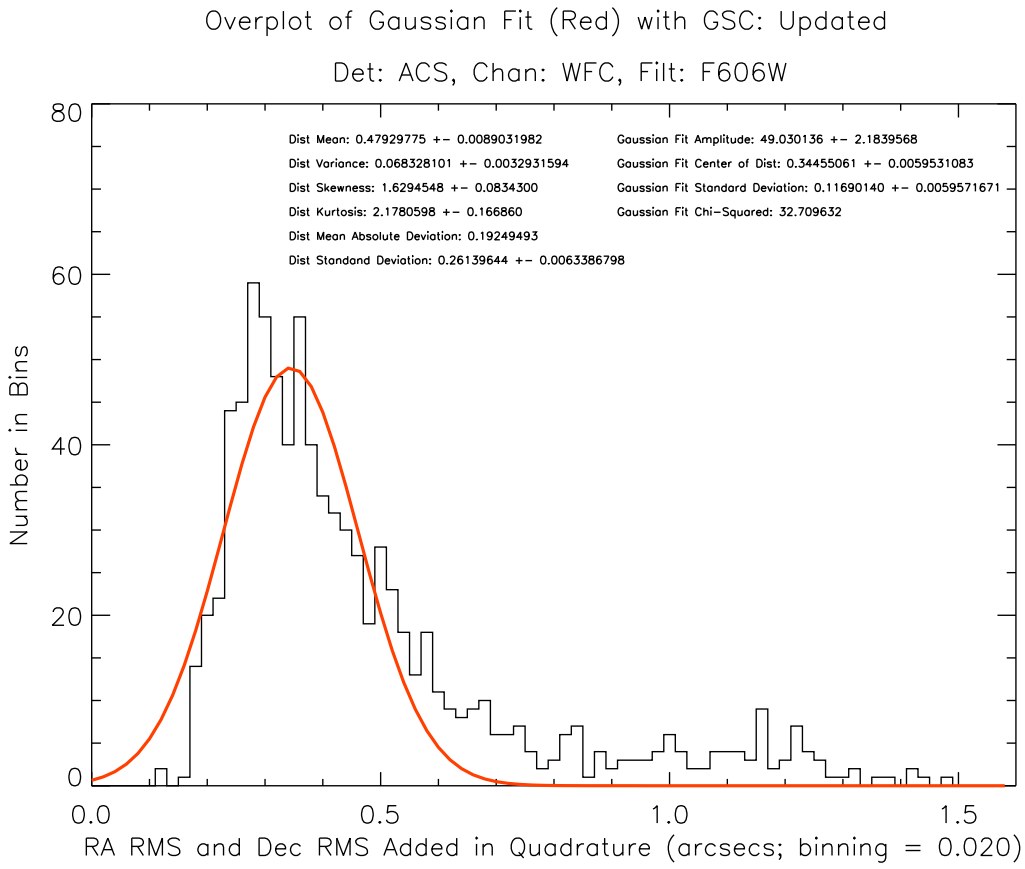

Fig. 15.— This plot shows the right ascension and declination RMSs added in quadrature. F606W was used to make this histogram.

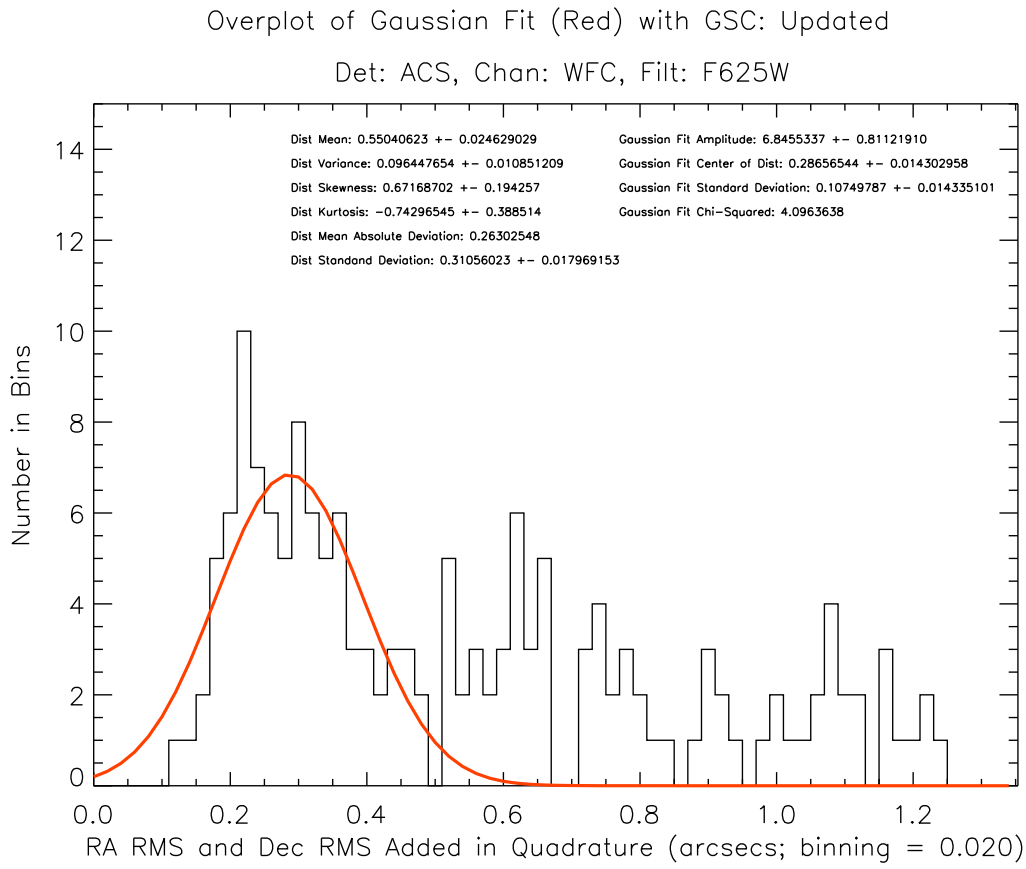

Fig. 16.— This plot shows the right ascension and declination RMSs added in quadrature. F625W was used to make this histogram.

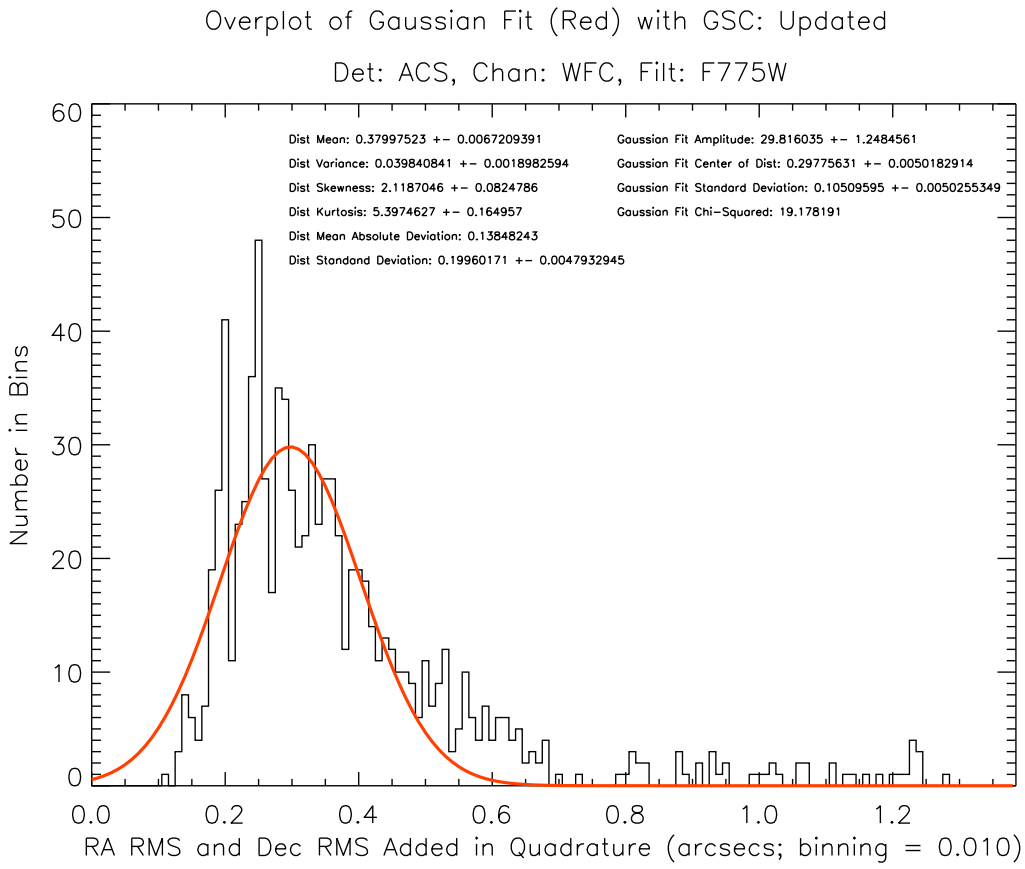

Fig. 17.— This plot shows the right ascension and declination RMSs added in quadrature. F775W was used to make this histogram.

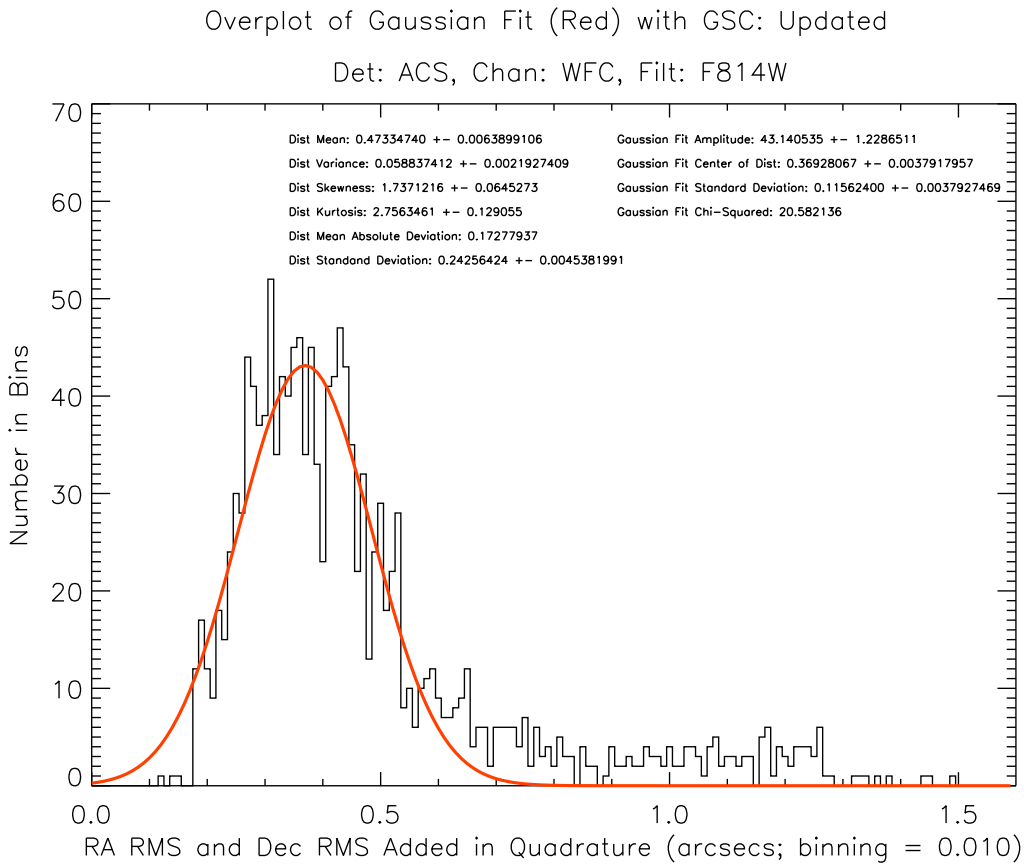

Fig. 18.— This plot shows the right ascension and declination RMSs added in quadrature. F814W was used to make this histogram.

7.2. ACS: Plot of a Gaussian Fit to the Total RMSs Derived from SDSS

In the subsequent histograms the peaks have RMS values which are derived from SDSS. There are two columns of statistics in the legend of this figure which describes the properties of the distribution itself (first column) and describes the properties of the Gaussian fit to the distribution (second column). The total RMS value is 0.1414″ for SDSS.

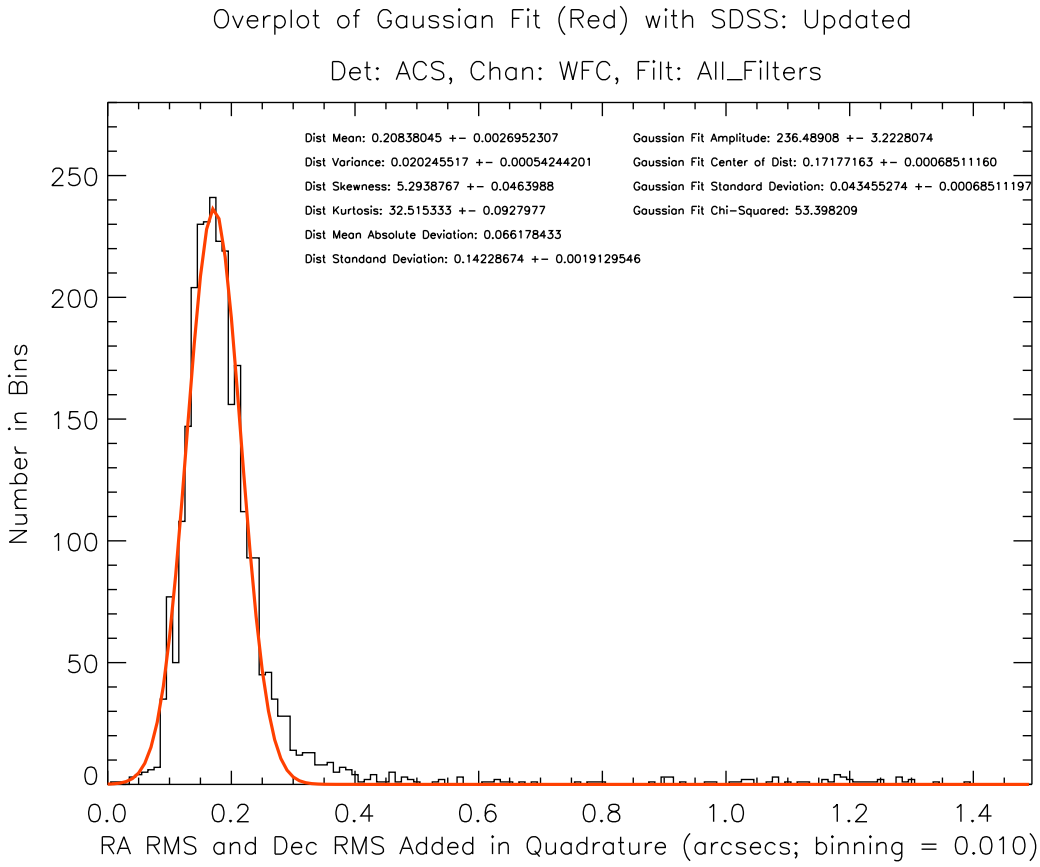

Fig. 19.— This plot shows the right ascension and declination RMSs added in quadrature. All filters were used to make this histogram.

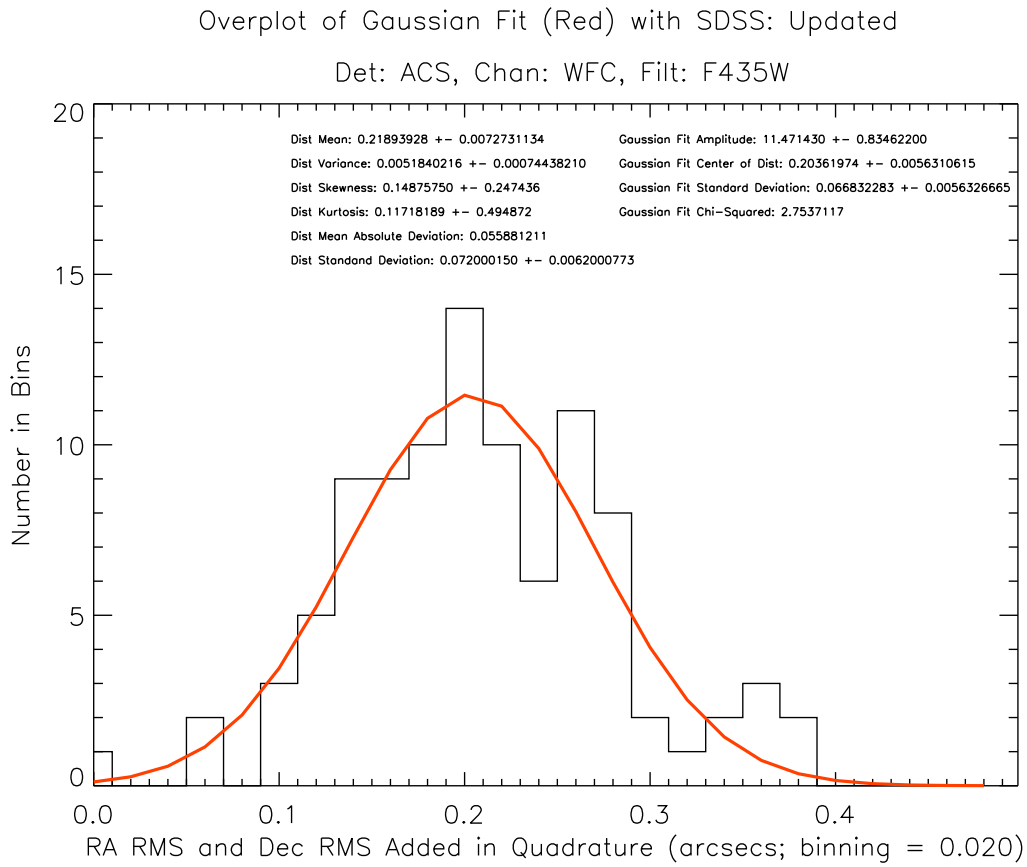

Fig. 20.— This plot shows the right ascension and declination RMSs added in quadrature. F435W was used to make this histogram.

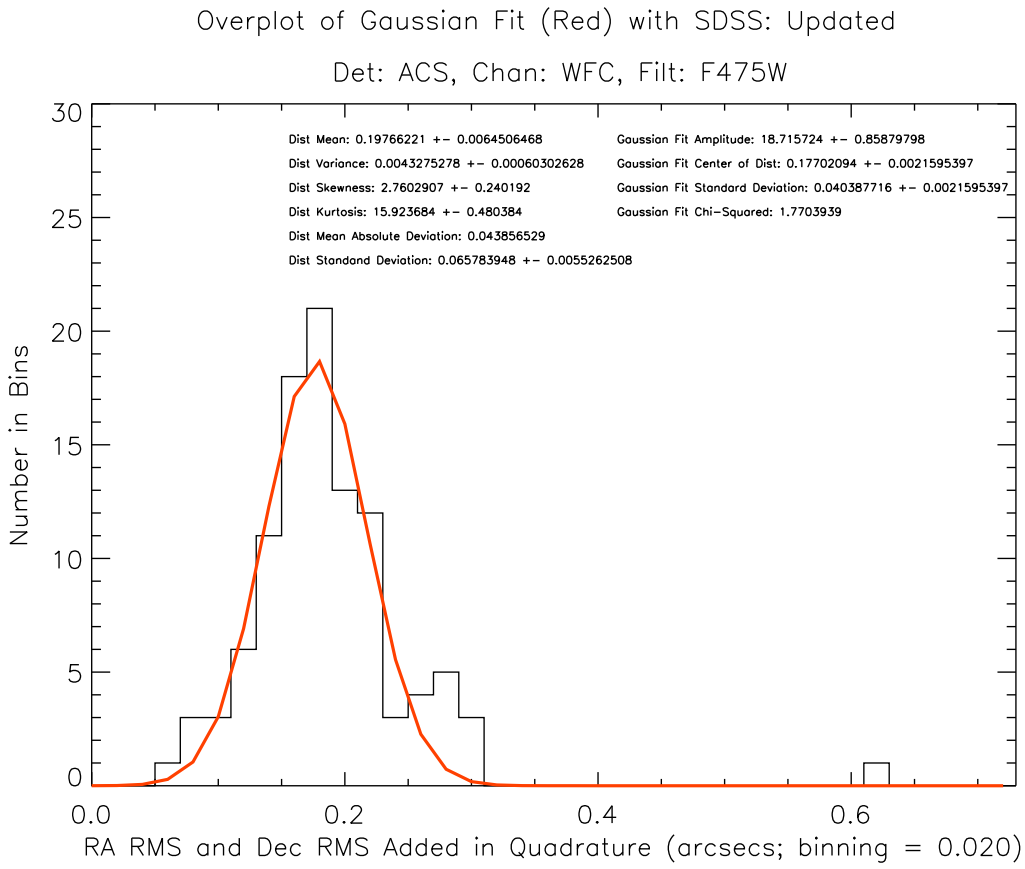

Fig. 21.— This plot shows the right ascension and declination RMSs added in quadrature. F475W was used to make this histogram.

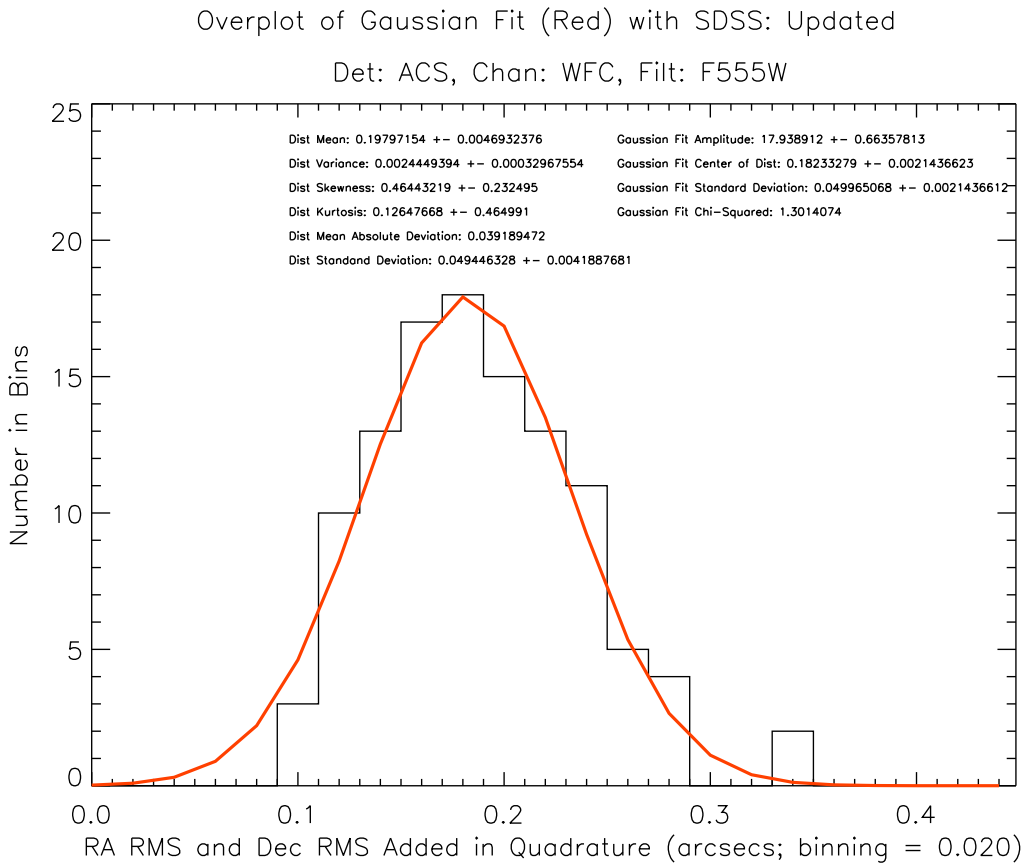

Fig. 22.— This plot shows the right ascension and declination RMSs added in quadrature. F555W was used to make this histogram.

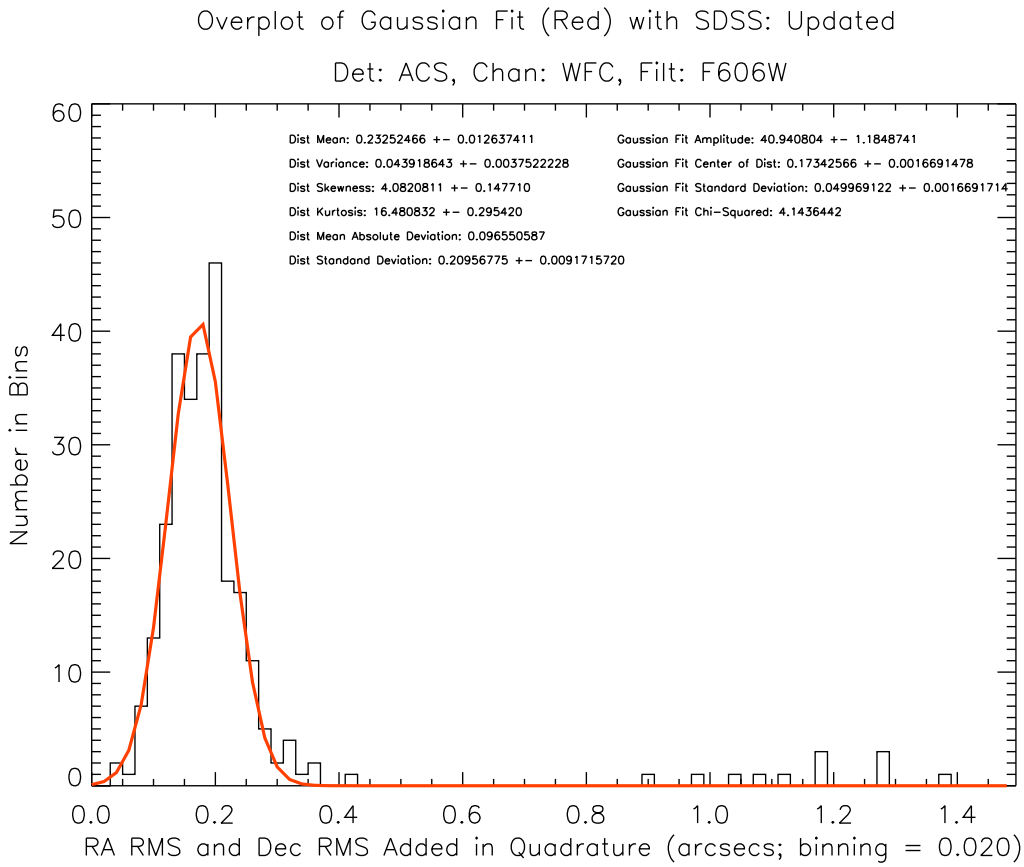

Fig. 23.— This plot shows the right ascension and declination RMSs added in quadrature. F606W was used to make this histogram.

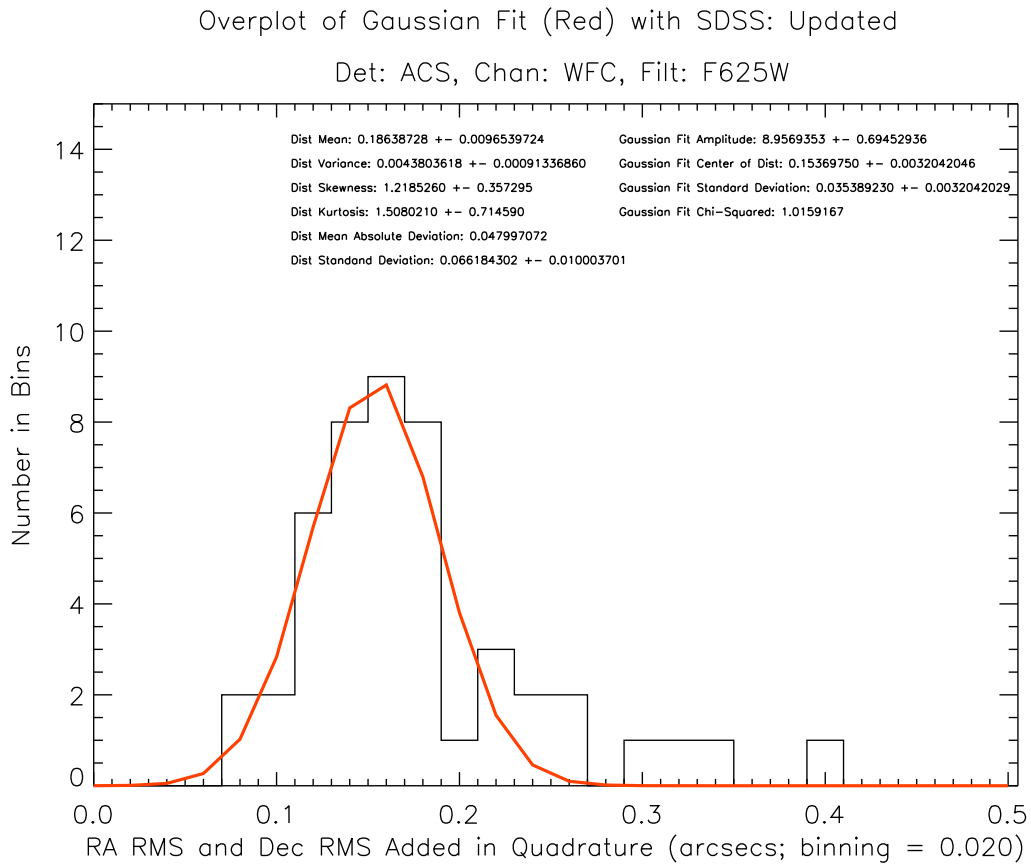

Fig. 24.— This plot shows the right ascension and declination RMSs added in quadrature. F625W was used to make this histogram.

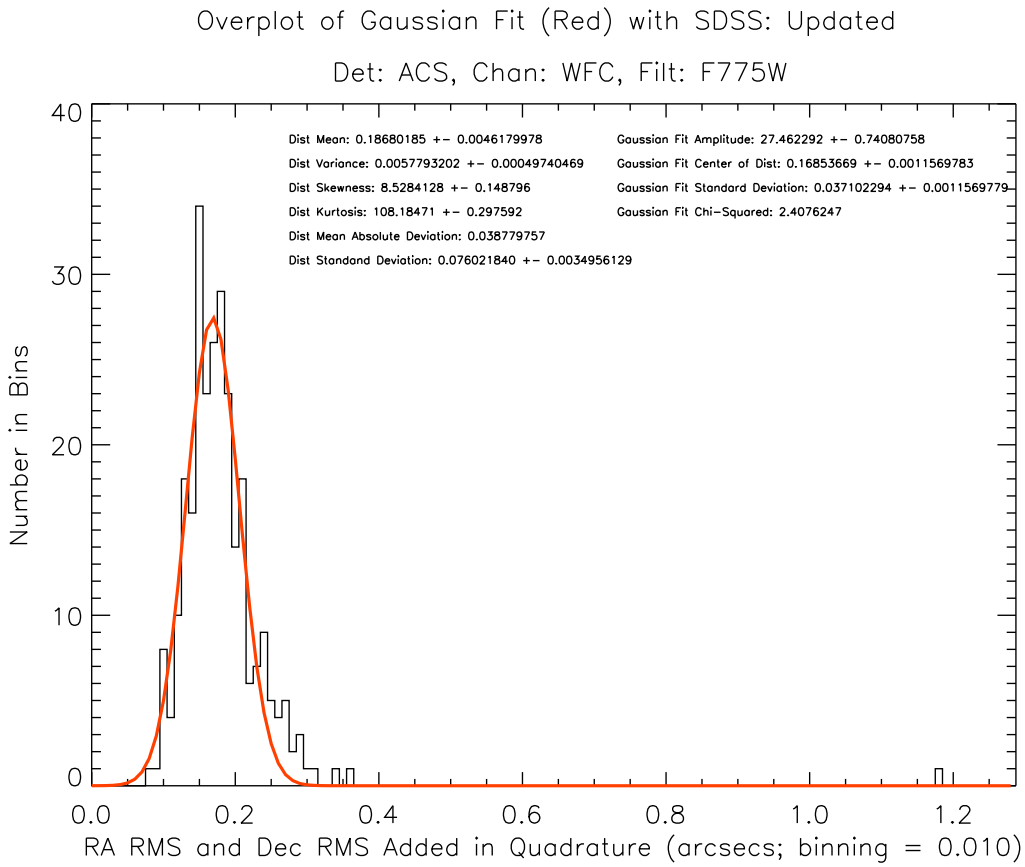

Fig. 25.— This plot shows the right ascension and declination RMSs added in quadrature. F775W was used to make this histogram.

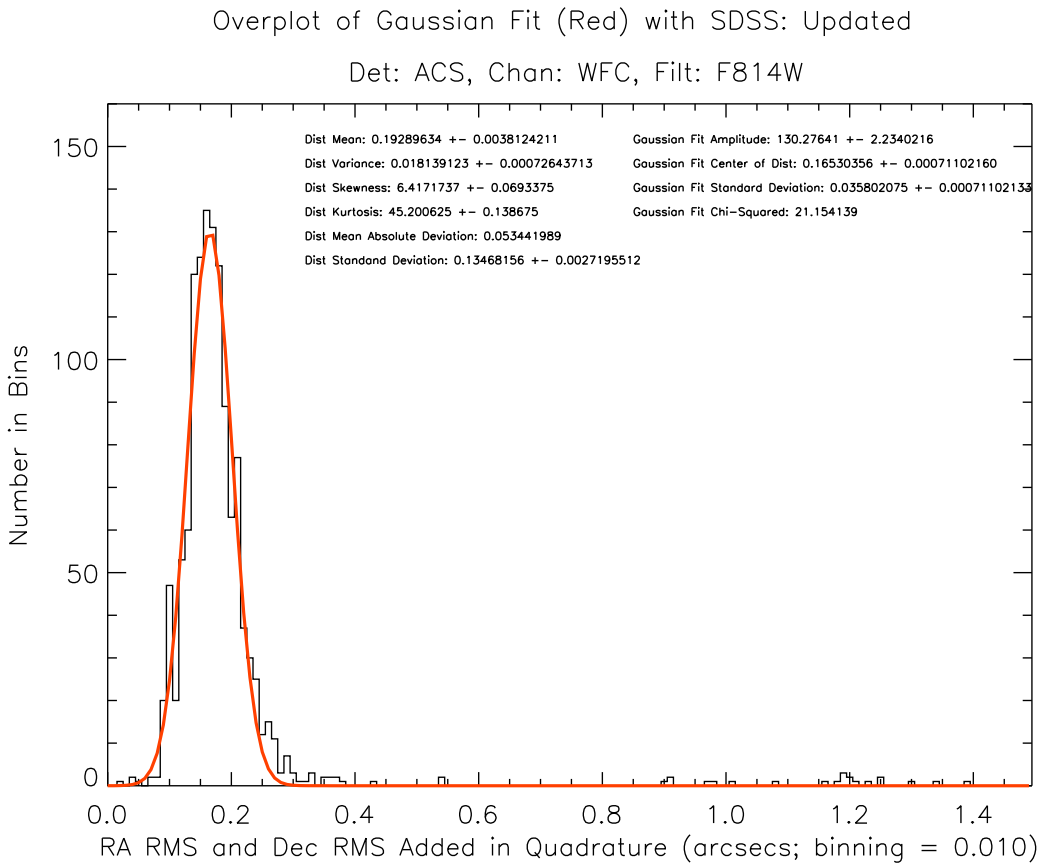

Fig. 26.— This plot shows the right ascension and declination RMSs added in quadrature. F814W was used to make this histogram.

7.3. WFPC2: Plot of a Gaussian Fit to the Total RMSs Derived from GSC II

In the subsequent histograms the peaks have RMS values which are derived from GSC II. There are two columns of statistics in the legend of this figure which describes the properties of the distribution itself (first column) and describes the properties of the Gaussian fit to the distribution (second column). The total RMS range is between 0.2828″ and 0.3960″ for GSC II.

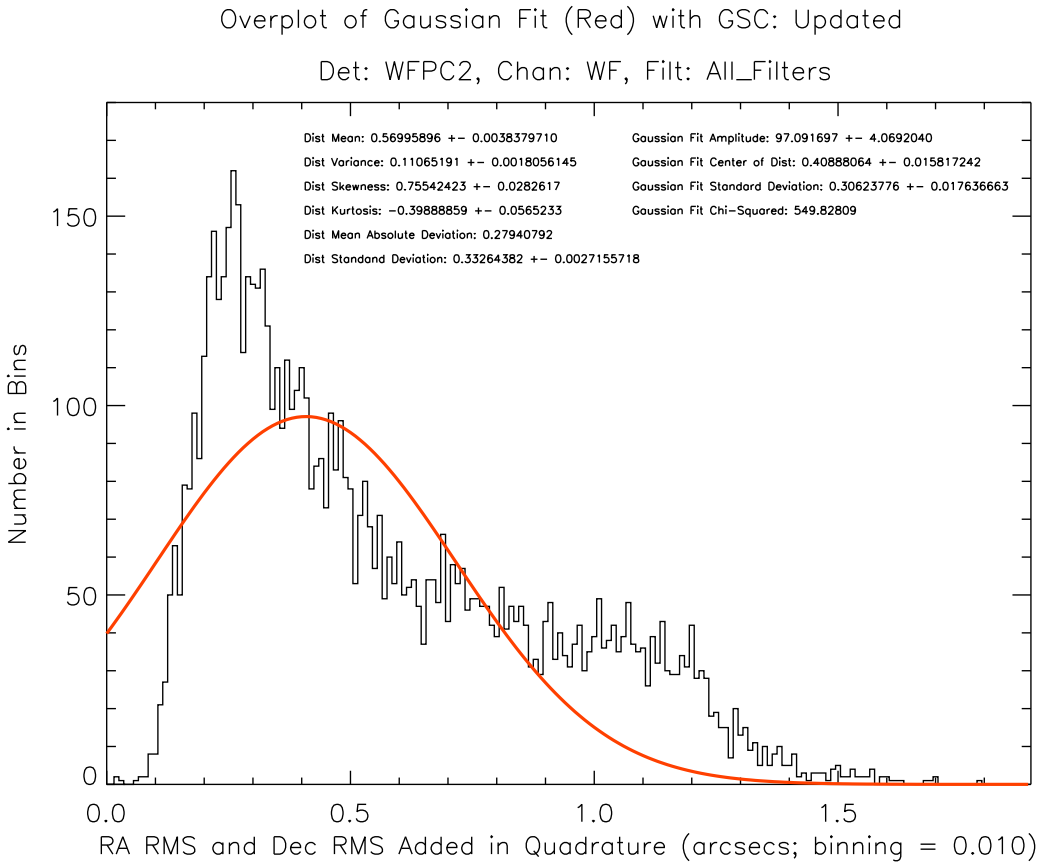

Fig. 27.— This plot shows the right ascension and declination RMSs added in quadrature. All filters were used to make this histogram.

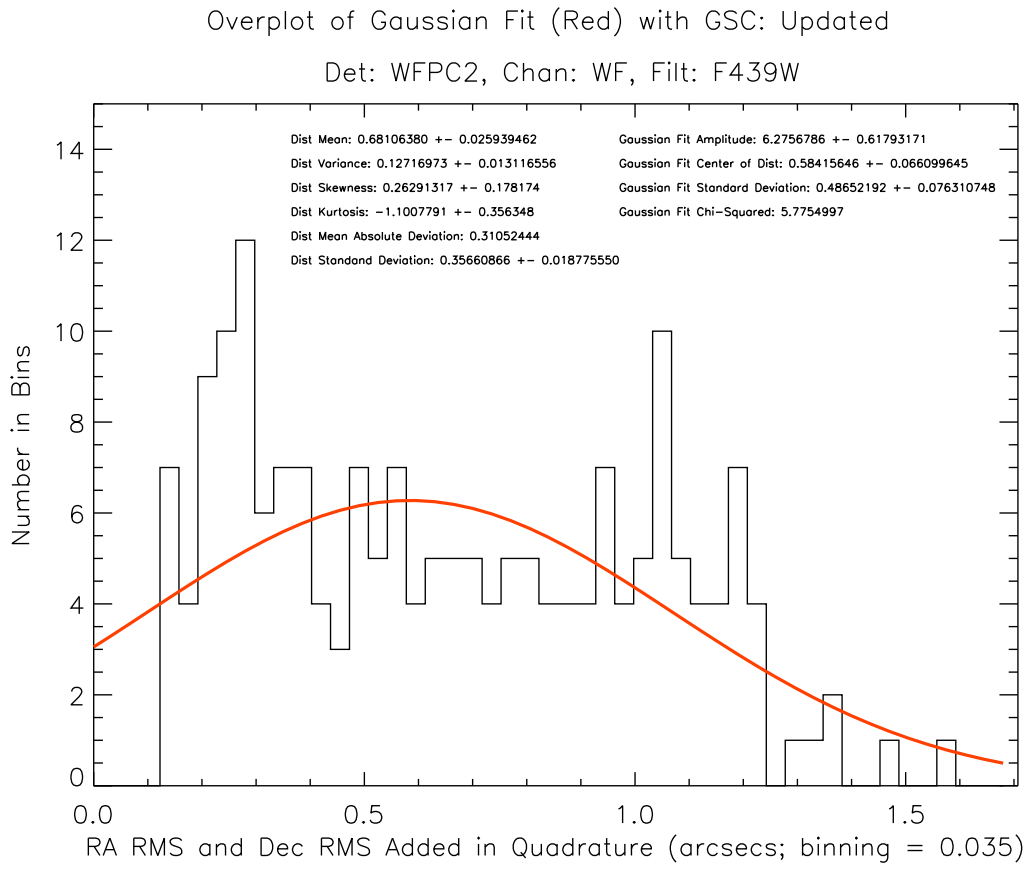

Fig. 28.— This plot shows the right ascension and declination RMSs added in quadrature. F439W was used to make this histogram.

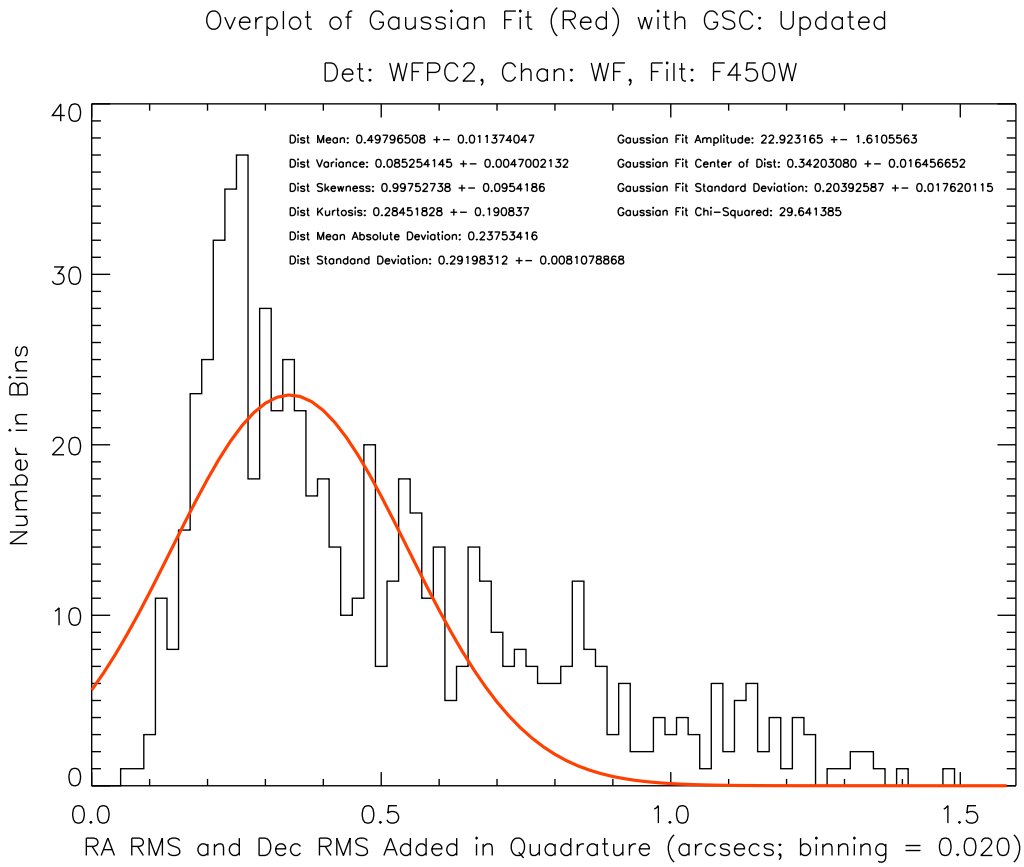

Fig. 29.— This plot shows the right ascension and declination RMSs added in quadrature. F450W was used to make this histogram.

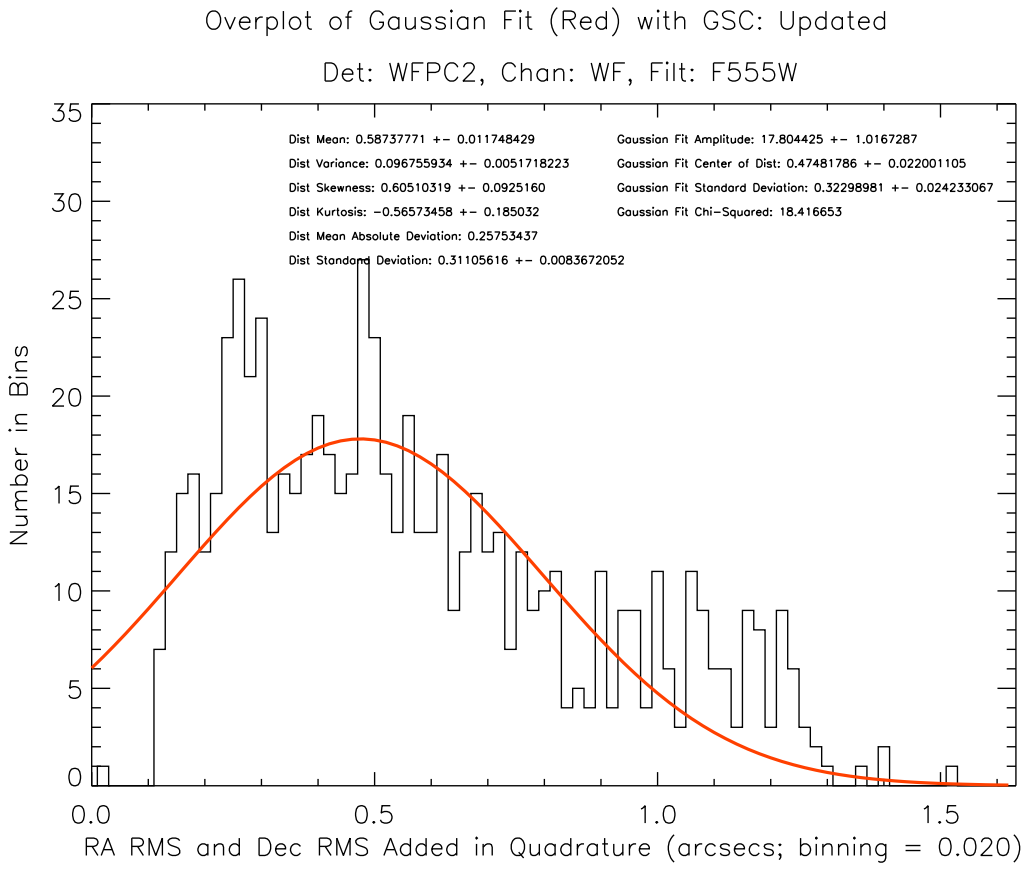

Fig. 30.— This plot shows the right ascension and declination RMSs added in quadrature. F555W was used to make this histogram.

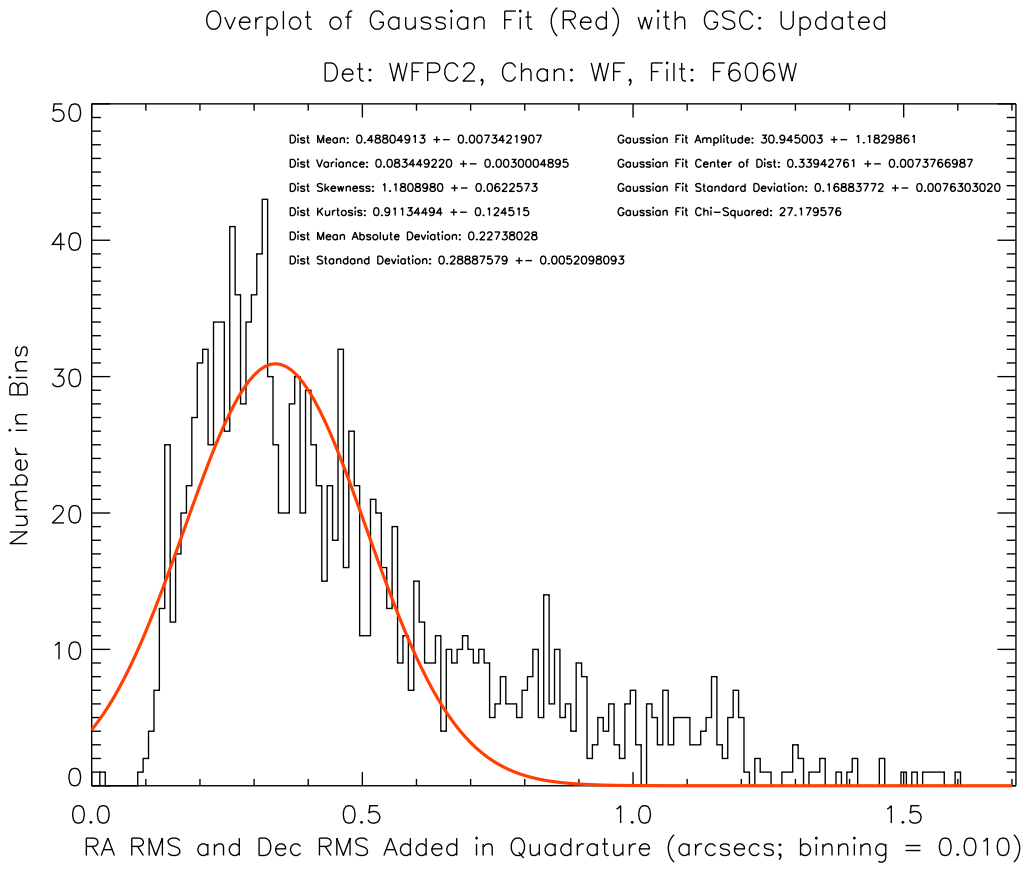

Fig. 31.— This plot shows the right ascension and declination RMSs added in quadrature. F606W was used to make this histogram.

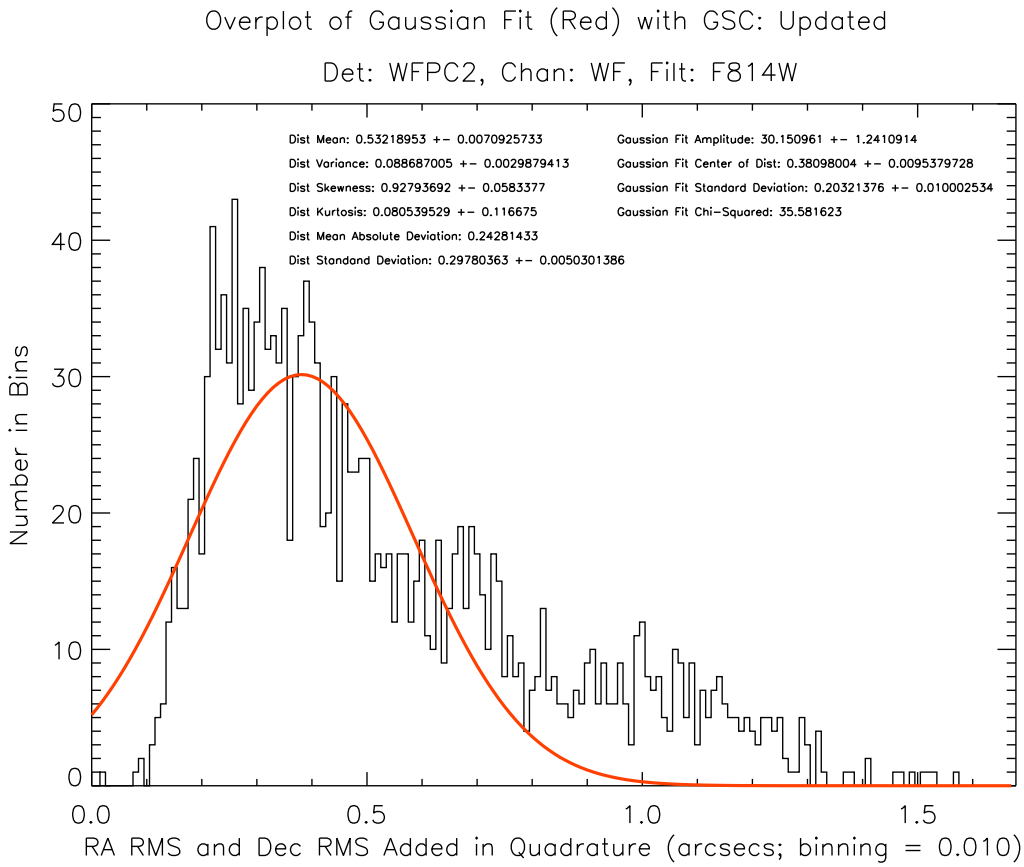

Fig. 32.— This plot shows the right ascension and declination RMSs added in quadrature. F814W was used to make this histogram.

7.4. WFPC2: Plot of a Gaussian Fit to the Total RMSs Derived from SDSS

In the subsequent histograms the peaks have RMS values which are derived from SDSS. There are two columns of statistics in the legend of this figure which describes the properties of the distribution itself (first column) and describes the properties of the Gaussian fit to the distribution (second column). The total RMS value is 0.1414″ for SDSS.

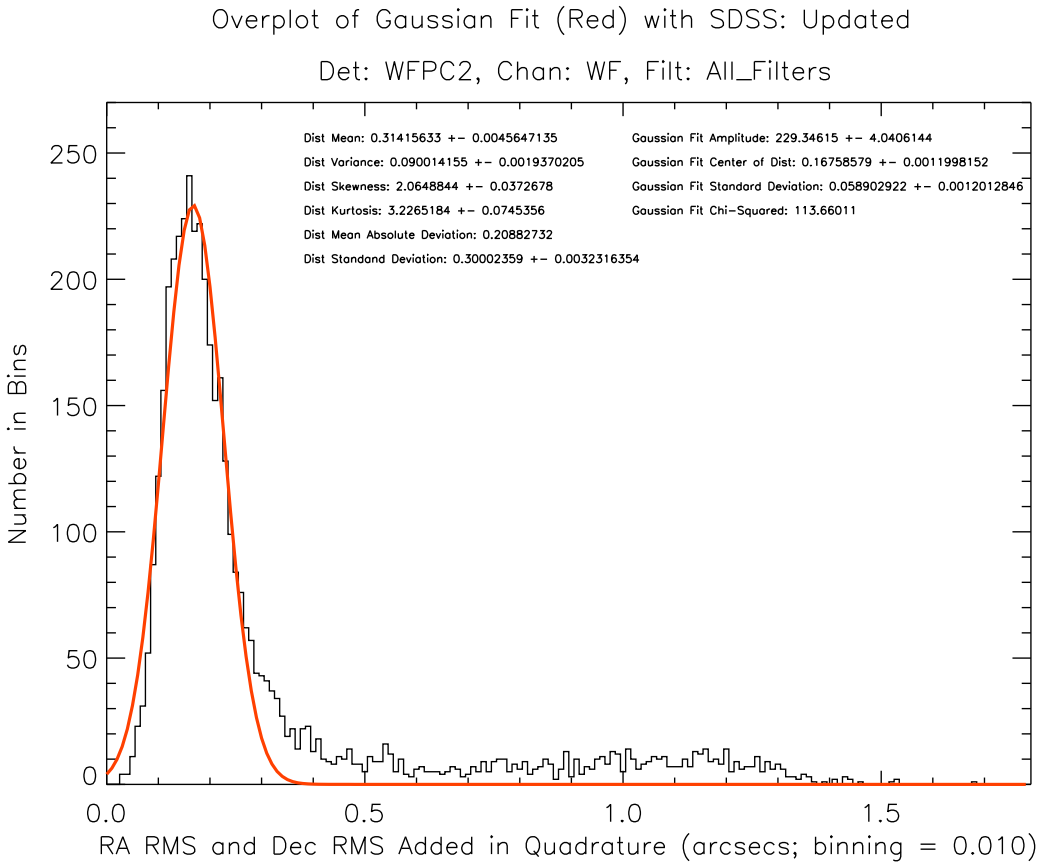

Fig. 33.— This plot shows the right ascension and declination RMSs added in quadrature. All filters were used to make this histogram.

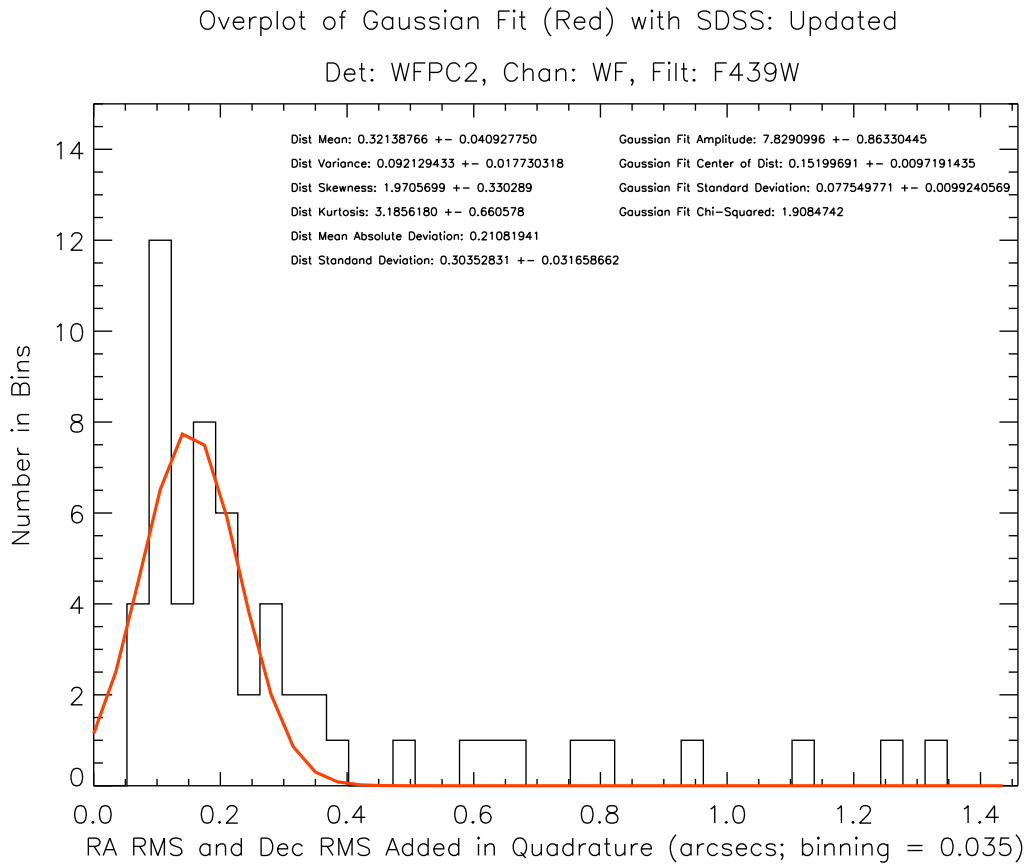

Fig. 34.— This plot shows the right ascension and declination RMSs added in quadrature. F439W was used to make this histogram.

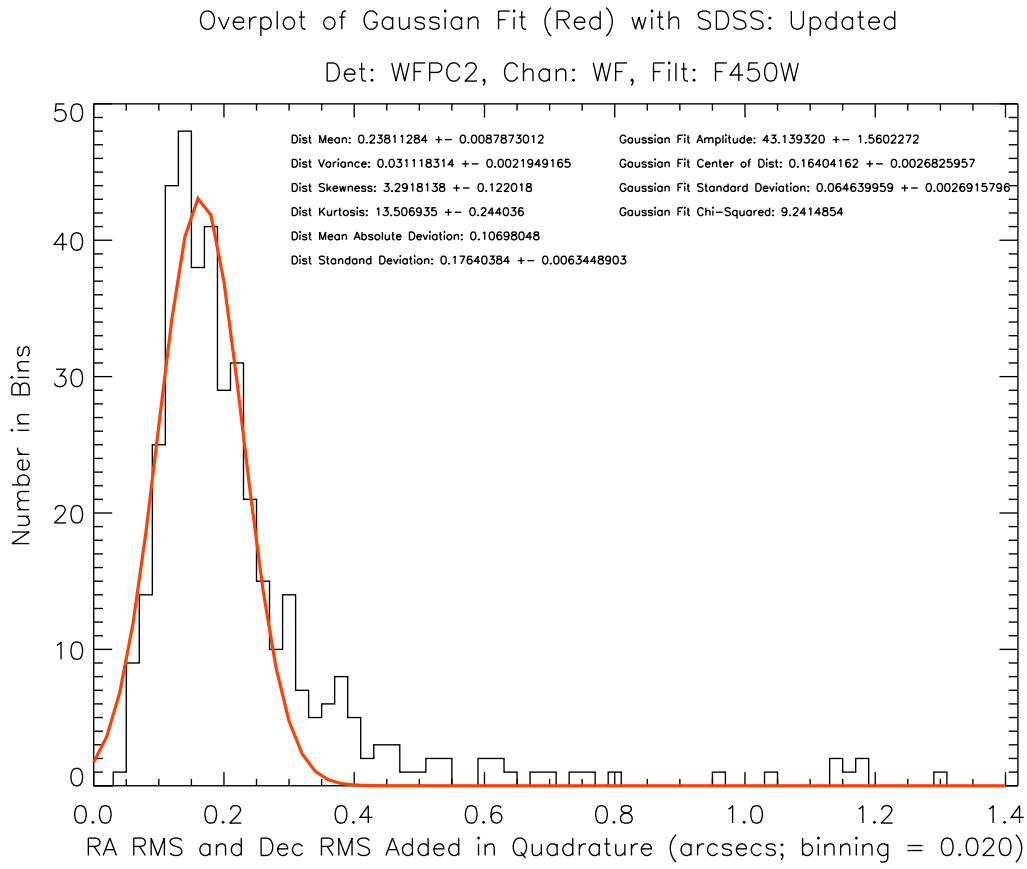

Fig. 35.— This plot shows the right ascension and declination RMSs added in quadrature. F450W was used to make this histogram.

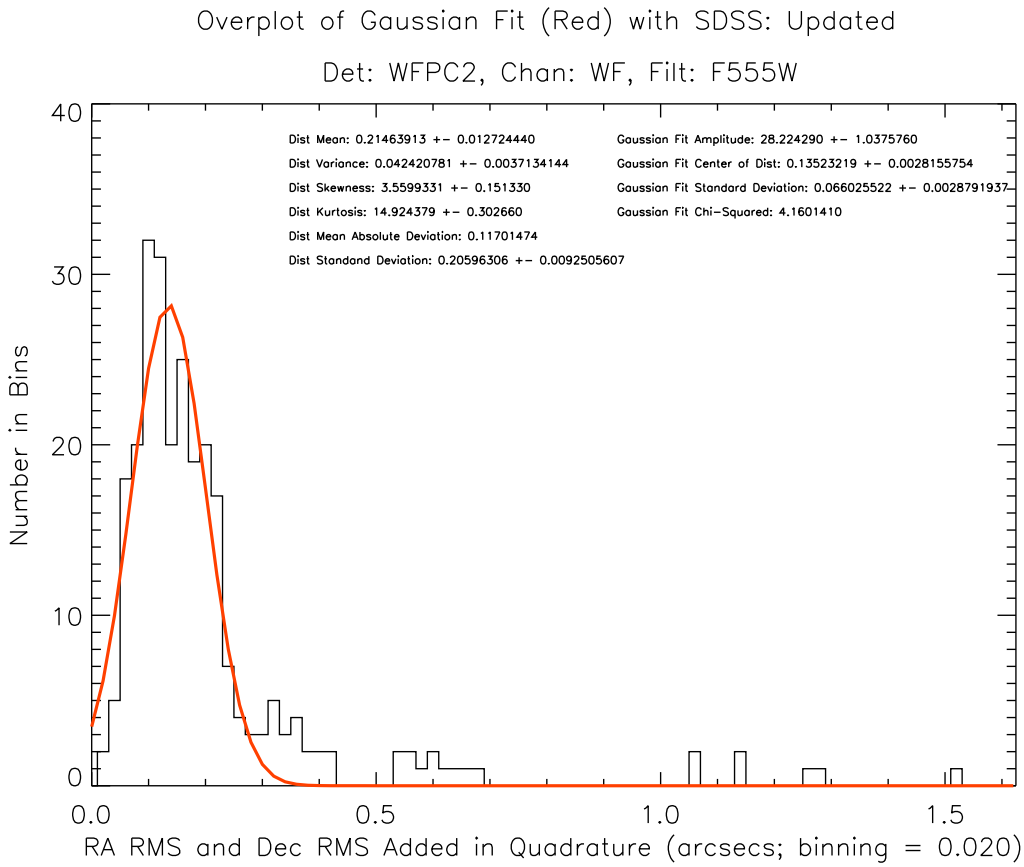

Fig. 36.— This plot shows the right ascension and declination RMSs added in quadrature. F555W was used to make this histogram.

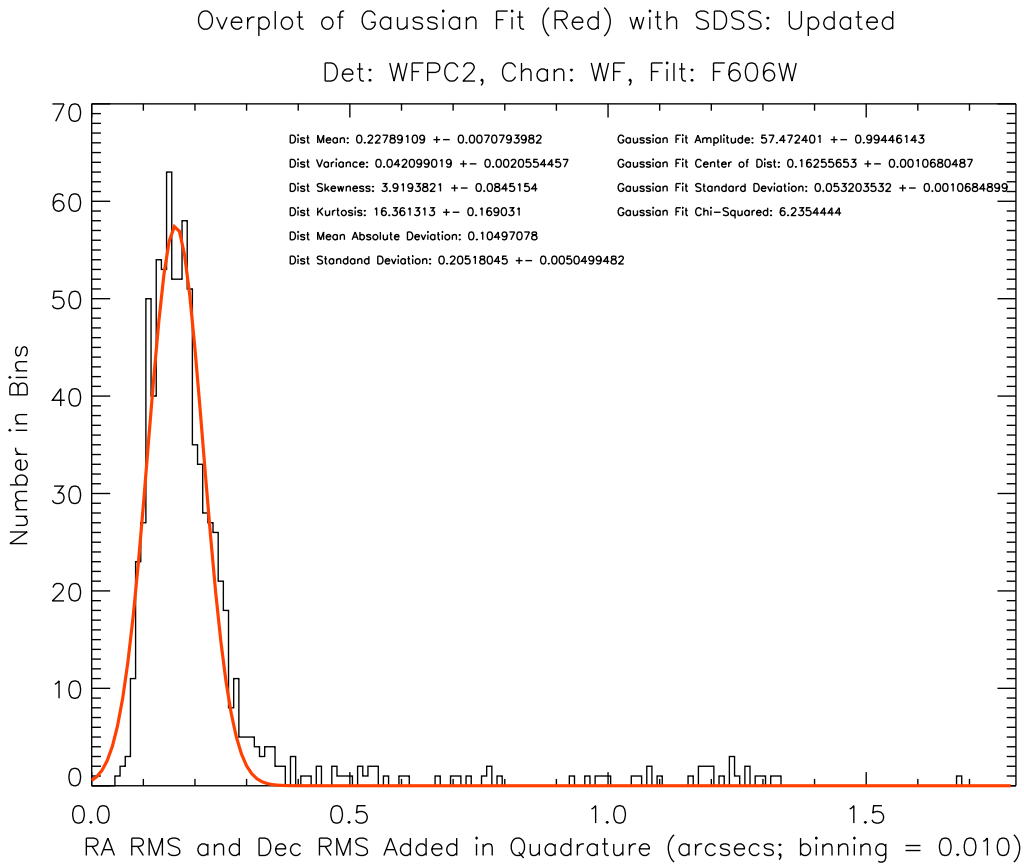

Fig. 37.— This plot shows the right ascension and declination RMSs added in quadrature. F606W was used to make this histogram.

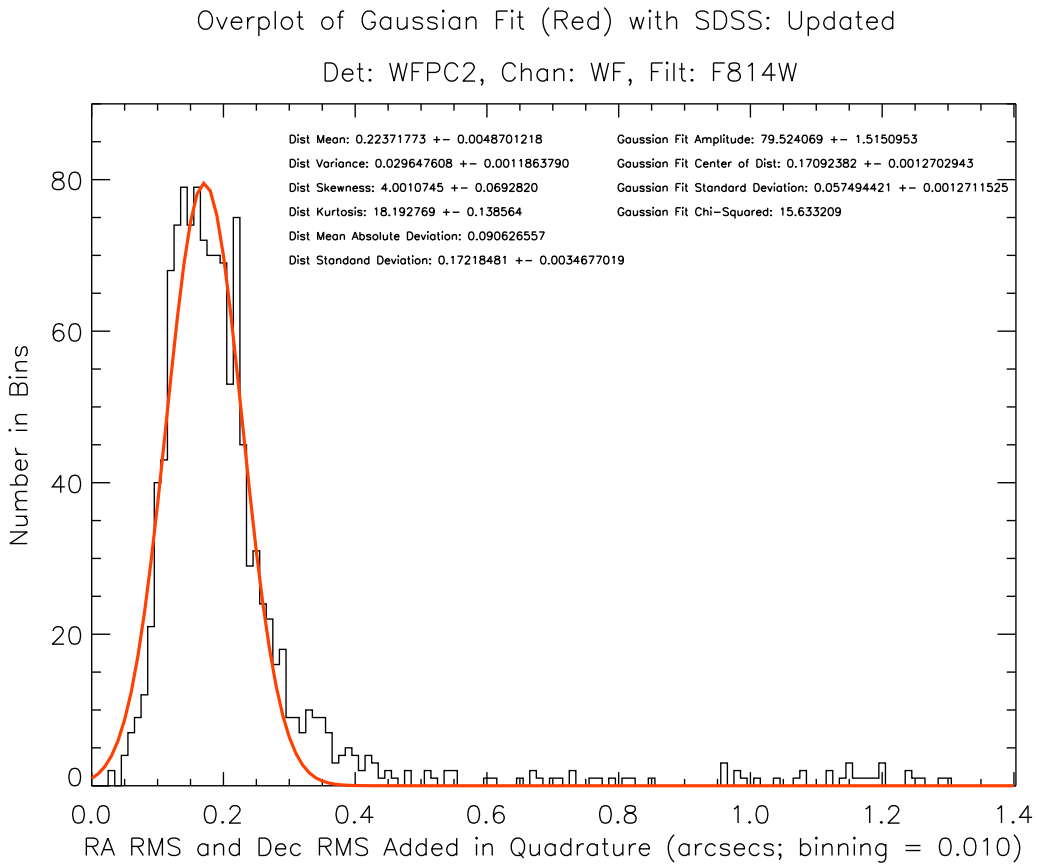

Fig. 38.— This plot shows the right ascension and declination RMSs added in quadrature. F814W was used to make this histogram.

7.5. Throughput Filter Curves

The following plots portray throughput curves for SDSS and ACS throughputs and GSC II and WFPC2 throughputs.

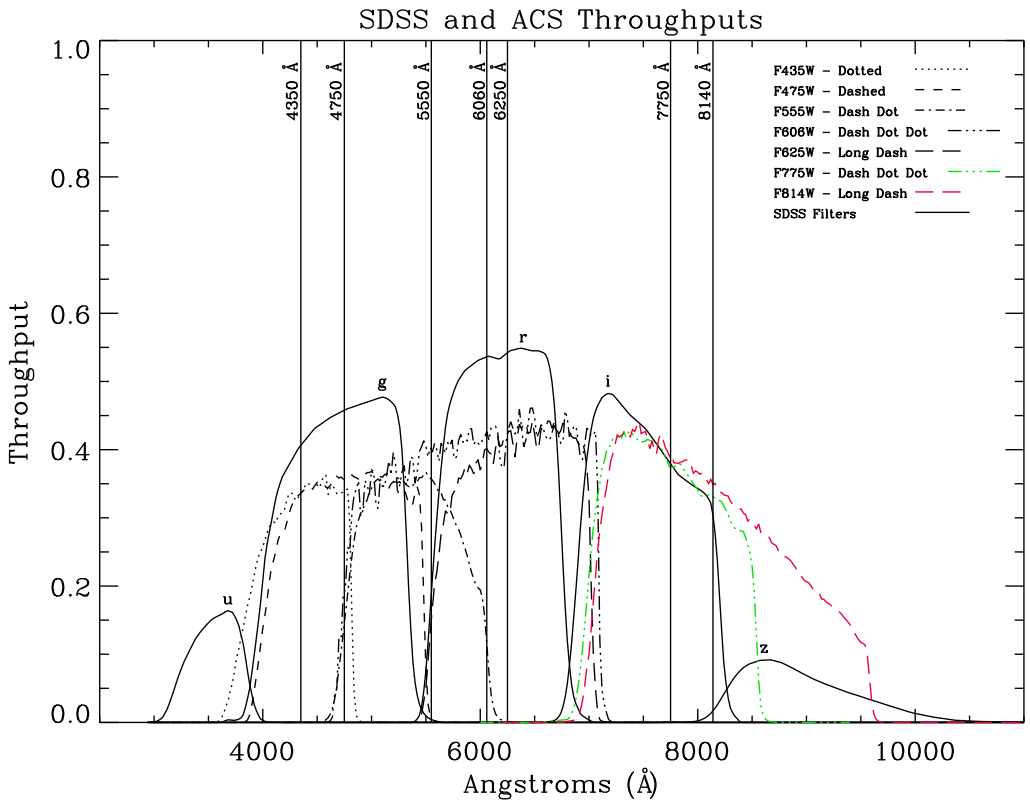

Fig. 39.— This figure portrays a comparison of SDSS and ACS throughput filter curves. The legend in the plot describes what each throughput curve represents. The vertical lines show the approximate effective wavelength.

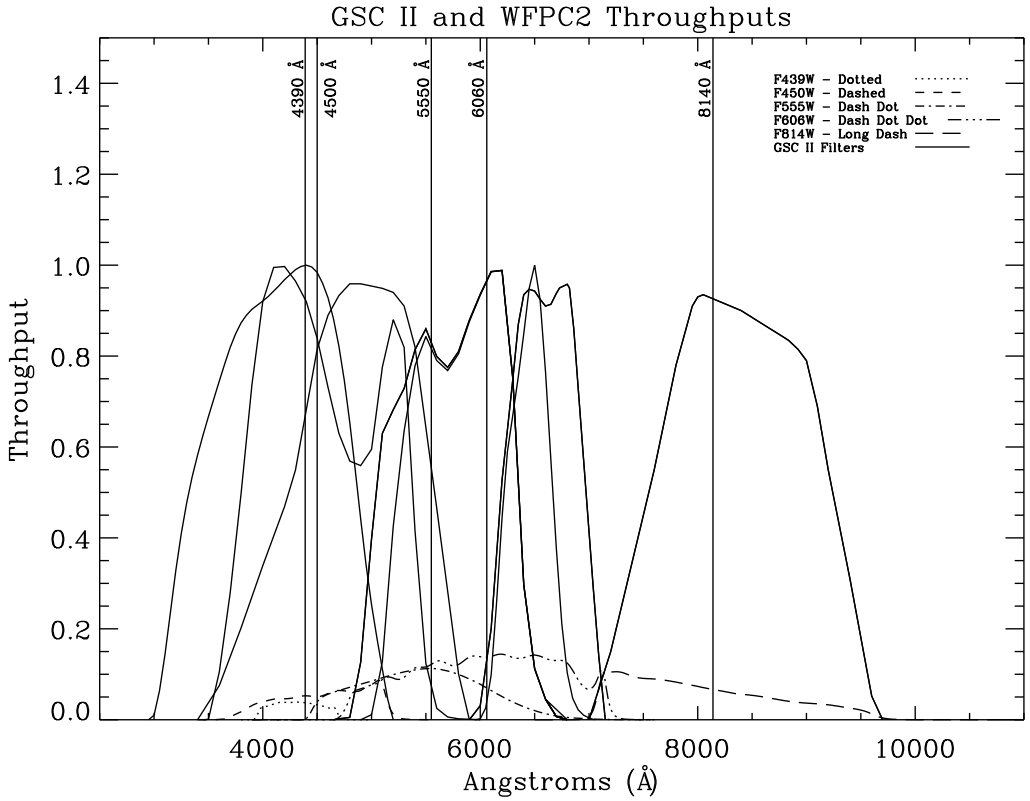

Fig. 40.— This figure portrays a comparison of GSC II and WFPC2 throughput filter curves. The legend in the plot describes what each throughput curve represents. The vertical lines show the approximate effective wavelength.